
Towards Unsupervised Domain Bridging via Image Degradation in Semantic Segmentation

Wangkai Li¹, Rui Sun¹, Huayu Mai¹, Tianzhu Zhang^{1,2*}

¹MoE Key Laboratory of Brain-inspired Intelligent Perception and Cognition,
University of Science and Technology of China

²National Key Laboratory of Deep Space Exploration, Deep Space Exploration Laboratory
{lwklwk, issunrui, mai556}@mail.ustc.edu.cn, tzzhang@ustc.edu.cn

Abstract

Semantic segmentation suffers from significant performance degradation when the trained network is applied to a different domain. To address this issue, unsupervised domain adaptation (UDA) has been extensively studied. Despite the effectiveness of selftraining techniques in UDA, they still overlook the explicit modeling of domain-shared feature extraction. In this paper, we propose DiDA, an unsupervised domain bridging approach for semantic segmentation. DiDA consists of two key modules: (1) Degradation-based Intermediate Domain Construction, which creates continuous intermediate domains through simple image degradation operations to encourage learning domain-invariant features as domain differences gradually diminish; (2) Semantic Shift Compensation, which leverages a diffusion encoder to disentangle and compensate for semantic shift information with degraded time-steps, preserving discriminative representations in the intermediate domains. As a plug-and-play solution, DiDA supports various degradation operations and seamlessly integrates with existing UDA methods. Extensive experiments on multiple domain adaptive semantic segmentation benchmarks demonstrate that DiDA consistently achieves significant performance improvements across all settings. Code is available at <https://github.com/Woof6/DiDA>.

1 Introduction

Semantic segmentation, a fine-grained pixel-wise classification task, assigns semantic class labels to each pixel, facilitating high-level image analysis. Despite the remarkable progress made in this field [56, 6, 18, 17], networks trained within source domain often encounter significant performance degradation when applied to a target dataset due to domain discrepancies. Mitigating this issue to enhance the generalization capability of networks remains a formidable challenge. To address this problem, extensive research has resorted to unsupervised domain adaptation (UDA), which aims to transfer knowledge from a labeled source domain to an unlabeled target domain.

In previous works, to fully exploit the abundance of unlabeled target domain data, self-training techniques have been naturally incorporated into UDA tasks and have emerged as a mainstream paradigm. The core idea of this paradigm lies in constructing a teacher network via temporal ensembling mechanisms, which generates pseudo-labels by predicting the target domain images. These pseudo-labels are then used to progressively guide the student network’s learning on the target domain. Despite achieving impressive results, these methods still overlook the explicit modeling of domain-shared feature extraction, which remains a central challenge in UDA. To illustrate this, we refer to the classic notion of causal representation learning [36, 74]: any observed feature can be generated as $x = \Phi(c, e)$, where Φ is a generator, c denotes the causal feature that determines

*Corresponding author

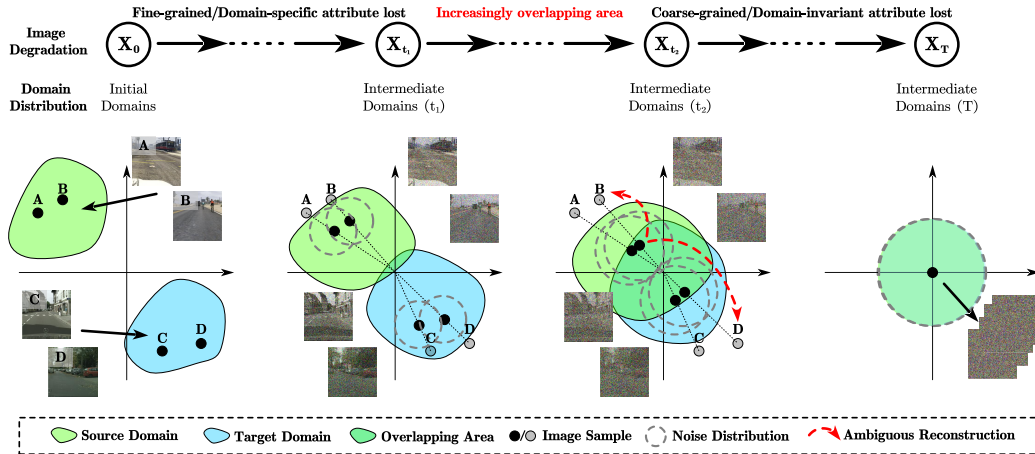


Figure 1: Conceptual illustration of the diffusion forward process. Fine-grained, domain-specific attributes such as texture are lost with less noise added (i.e., early time-steps), while coarse-grained, domain-invariant ones such as shape are lost by adding more noise (i.e., late time-steps).

the domain-invariant class identity (e.g., shape), and e represents the environment-specific feature (e.g., texture). Since environmental features are domain-specific, the domain shift $e_S \neq e_T$ leads to $x_S \neq x_T$, thereby hindering the learning of a truly domain-invariant class representation.

In this work, we explore a novel perspective for unsupervised domain bridging and demonstrate that simple image degradation operations can serve as effective priors. Our key idea is motivated by the theoretical insight (Sec.3.2) of the Denoising Diffusion Probabilistic Model (DM) [37, 76]. As shown in Fig. 1, the forward diffusion process incrementally adds Gaussian noise to input samples at each time step. This process gradually removes domain-specific attributes, effectively collapsing samples from different domains into a shared representation space. As the time step increases, this diffusion process enlarges the overlapping area of the probability density functions of the noisy domain distributions. Existing studies [95, 77] show that this overlapping area is closely correlated with the DM’s ambiguous reconstruction of different samples. For instance, due to the large overlap between the intermediate distributions at a certain time step t_2 , noisy samples drawn from these may be reconstructed ambiguously as either source domain or target domain. This observation leads to a crucial insight: the overlapping area formed through degradation can be interpreted as a domain-shared distribution, which acts as a valuable prior for learning domain-invariant representations. This hypothesis is further substantiated by our quantitative analysis presented in Appendix H, where we empirically validate the correlation between degradation level and domain alignment effectiveness.

It is non-trivial to interpret image degradation as a form of domain bridging, especially considering its fundamental differences from consistency regularization based on data augmentation [40, 93]. This perspective introduces two major challenges: (1) **Wide Range of Degradation Levels:** Degradation operations, when applied incrementally from mild to severe, can gradually eliminate domain-specific attributes. To effectively capture domain-invariant information under such conditions, the encoder of the segmentation network should maintain stable and consistent feature representations across varying levels of degradation. (2) **Semantic Shift Due to Feature Corruption:** While degradation helps remove domain-specific cues, it also inevitably affects domain-invariant features. This degradation of essential semantic information hinders the encoder’s ability to extract discriminative representations, which in turn compromises the learning process of the segmentation head. This issue is commonly referred to as the semantic shift problem [1, 86].

To this end, we propose an unsupervised domain bridging approach for semantic segmentation, termed DiDA, which constructs intermediate domains via image degradation defined by a forward diffusion process. We introduce the following key components to integrate DiDA into the UDA training pipeline: (1) **Degradation-based Intermediate Domain Construction:** Based on the definition of the forward diffusion process, we construct a sequence of continuous intermediate domains through simple image degradation operations. These intermediate domains are incorporated into the UDA training process to encourage the model to learn more domain-invariant features from the increasingly overlapping area of domain distributions. (2) **Semantic Shift Compensation:** To mitigate the

semantic shift problem introduced during intermediate domain construction, we propose a diffusion encoder, conditioned on a time embedding module. This encoder disentangles the time-specific semantic shift and, through residual connections across multiple feature levels, compensates for the lost discriminative representations in intermediate domains. This ensures better semantic alignment between extracted features and corresponding labels. (3) **Expansion to Arbitrary Degradation:** To demonstrate the flexibility of our framework, we explore various degradation operations for constructing intermediate domains. The implementation of DiDA is compatible with any image degradation method by simply replacing the Gaussian noise addition in the standard diffusion process. This characteristic showcases the generality and extensibility of our framework. Our approach can be regarded as a plug-and-play training strategy, which can be seamlessly integrated with various UDA methods and network architectures, consistently yielding performance improvements.

In this work, our contributions can be summarized as follows: (1) We propose a novel domain bridging mechanism based on image degradation to facilitate the learning of domain-invariant features. This introduces a new perspective for domain-adaptive semantic segmentation. (2) We design a unified framework that integrates diffusion strategies into the training pipeline of UDA. By introducing a series of degradation-based intermediate domains, our approach enables progressive learning of domain-invariant representations and effectively mitigates the semantic shift problem commonly observed in intermediate domains. (3) We validate the effectiveness and versatility of our approach through extensive experiments on multiple UDA methods, benchmarks, and network architectures. DiDA consistently achieves significant performance improvements across all settings.

2 Related Work

2.1 Unsupervised Domain Adaptation (UDA)

Unsupervised Domain Adaptation (UDA) aims to transfer semantic knowledge from labeled source domains to unlabeled target domains. Given widespread domain gaps [88, 67], UDA has been extensively studied across various vision tasks, including image classification [29, 28, 57, 35, 34], object detection [11, 12, 51], and semantic segmentation [83, 101, 98, 9]. Semantic segmentation requires assigning a label to each pixel, which often leads to high annotation costs [13, 52, 87]. To address this, various label-efficient methods have been developed, such as semi-supervised learning [79, 62, 78], few-shot learning [54, 59, 55, 53], and domain adaptation [49, 15, 14]. Among them, UDA is particularly valuable, as it eliminates the need for costly pixel-level annotations in new domains. Recent UDA methods for semantic segmentation fall into two main categories: adversarial training and self-training. Adversarial methods align source and target feature distributions via a min-max game between a feature extractor and a domain discriminator [81, 83]. Self-training methods, gaining traction due to the domain-robustness of Transformers [4], adopt a teacher-student framework to generate pseudo labels for target images [82, 38, 60, 50]. Their success hinges on producing reliable pseudo labels through entropy minimization [8], consistency regularization [40], and class-balanced training [48]. Our method builds upon the self-training paradigm, introducing a novel domain bridging mechanism via image degradation to enhance domain invariance and improve adaptation performance.

2.2 Generative Models for Segmentation

Generative models like GANs [31] and VAEs [45] map data to latent codes following simple distributions (e.g., Gaussian), enabling data generation and manipulation. Denoising Diffusion Probabilistic Models (DDPMs) [37] extend this by modeling the data-to-latent mapping as a Markov chain with intermediate distributions. To adapt such generative mechanisms to semantic segmentation—a typically discriminative task—some works synthesize paired images and labels to train separate segmentation networks [47, 100], while others directly exploit internal features from generative models [91, 3, 80]. In domain adaptive segmentation, diffusion-based approaches have shown promise. Some methods leverage style transfer [68, 69] or generate diverse domain samples to enhance generalization [66, 99], while others estimate segmentation uncertainty to guide sample selection [26]. In contrast, our method integrates diffusion strategies into the UDA self-training framework, progressively learning domain-invariant representations from images sampled across intermediate distributions.

3 Methods

In this section, we first formalize the standard self-training paradigm for UDA and the training process for diffusion models, respectively (Sec.3.1). Then, we introduce theoretical insight (Sec.3.2). After that, we describe our new UDA framework, DiDA, a novel perspective for domain bridging that couples diffusion strategies to improve UDA semantic segmentation performance (Sec.3.3). Finally, we illustrate the details that expand our method to arbitrary choices of image degradation (Sec.3.4).

3.1 Preliminary Knowledge

Self-Training (ST) for UDA. For domain adaptive semantic segmentation, the source domain can be denoted as $D_s = \{(x_i^S, y_i^S)\}_{i=1}^{N_S}$, where $x_i^S \in X_S$ represents an image with $y_i^S \in Y_S$ as the corresponding pixel-wise one-hot label covering C classes. The target domain can be denoted as $D_t = \{(x_i^T)\}_{i=1}^{N_T}$, which shares the same label space but has no access to target label Y^T . In this setting, the supervised loss \mathcal{L}^S can be calculated on the source domain to train a neural network f_θ :

$$\mathcal{L}^S = \sum_{i=1}^{N_S} \mathcal{L}_{ce}(f_\theta(x_i^S), y_i^S, 1), \quad (1)$$

where \mathcal{L}_{ce} denotes the pixel-wise cross-entropy loss:

$$\mathcal{L}_{ce}(\hat{y}_i, y_i, q_i) = - \sum_{j=1}^{H \times W} \sum_{c=1}^C q(i, j, c) y(i, j, c) \log \hat{y}(i, j, c). \quad (2)$$

Self-training introduces a teacher-student framework to generate pseudo-labels p^T for the target domain (see Fig. 2): $p_{(i,j,c)}^T = [c = \operatorname{argmax}_{c'} f_\phi(x_i^S)_{(j,c')}]$, where f_ϕ is the teacher network. Then, the pseudo-labels are used to train the network f_θ on the target domain with the adaptation loss \mathcal{L}^T :

$$\mathcal{L}^T = \sum_{i=1}^{N_T} \mathcal{L}_{ce}(f_\theta(x_i^T), p_i^T, q^T). \quad (3)$$

The quality of pseudo-labels is weighted by a confidence estimate q^T [38], which gradually strengthens with increasing accuracy of models. After each training step, the teacher model f_ϕ is updated with the exponentially moving average of the weights of f_θ . The segmentation model, f_θ , can be defined as $f_\theta = h \circ g$, where $g: \mathcal{X} \rightarrow \mathcal{Z}$ is an encoder that lifts each pixel of the input image in \mathcal{X} to the feature space \mathcal{Z} , and $h: \mathcal{Z} \rightarrow \mathbb{R}^C$ is a segmentation head which can be viewed as a pixel-wise classifier to give a score for each class.

Diffusion Model. Diffusion models learn a series of state transitions to generate high-quality sample from the noise, defined as a forward diffusion process during the training phase. The diffusion process generates intermediate state x_t with a random uniformly sampled t from $\{1, \dots, T\}$:

$$q(x_t|x_0) = \mathcal{N}(x_t; \sqrt{\bar{\alpha}_t}x_0, (1 - \bar{\alpha}_t)\mathbf{I}), \quad (4)$$

where $\bar{\alpha}_t$ originates from a predefined noise schedule (decreases from 1 to 0). This process can be rewritten through a reparameterization trick:

$$x_t \triangleq \sqrt{\bar{\alpha}_t}x_0 + \sqrt{1 - \bar{\alpha}_t}\epsilon, \quad \epsilon \sim \mathcal{N}(0, \mathbf{I}). \quad (5)$$

Afterward, a network is trained to predict noise ϵ (or predict sample data x_0 directly) from x_t , with a reconstruction loss:

$$\mathcal{L}^R = \|f_\theta(x_t, t) - \epsilon\|_2^2. \quad (6)$$

3.2 Theoretical Insight

In the forward diffusion process, the loss of attributes with different levels of granularity is directly related to the time step. Specifically, we restate following proposition based on the findings in [95]:

Proposition (Attribute Loss and Time Step). 1) For each attribute Z_i , there exists a minimum time step $t(Z_i)$ such that Z_i is lost with degree τ at every $t \in \{t(Z_i), \dots, T\}$. 2) There exists a set $\{\beta_i\}_{i=1}^T$ such that $t(Z_i) > t(Z_j)$ whenever the distribution of $\|x_0 - g_i \cdot x_0\|$ first-order stochastically dominates that of $\|x_0 - g_j \cdot x_0\|$, where $x_0 \sim \mathcal{X}$ uniformly.

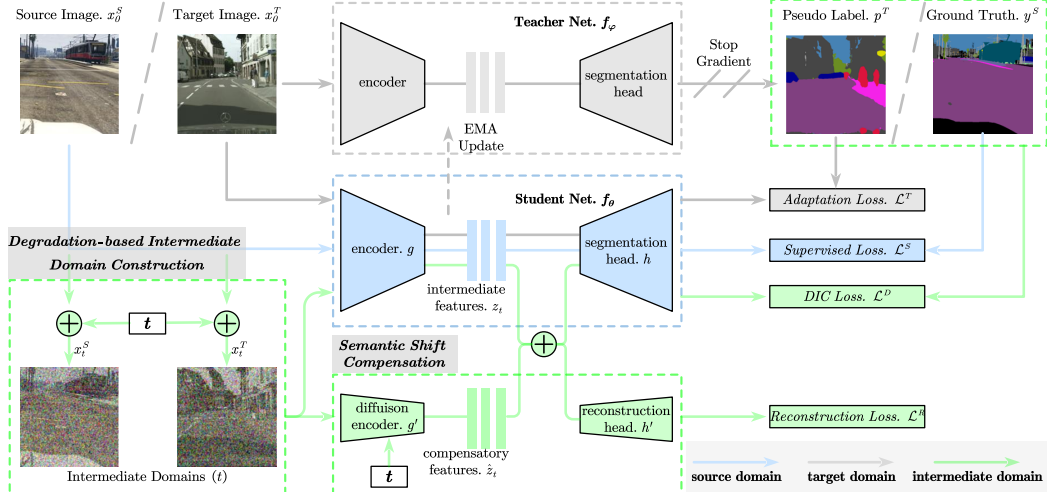


Figure 2: Overview of DiDA framework. We integrate diffusion strategies (green box) with a standard self-training paradigm. While regular frameworks train networks using supervised loss on source domain and unsupervised adaptation loss on target domain, DiDA introduces degradation-based intermediate domains and addresses semantic shift through a diffusion encoder and reconstruction head, which are enabled by degraded image consistency (DIC) loss and reconstruction loss.

The first part of the proposition indicates that once an attribute Z_i is lost at a certain time step $t(Z_i)$ with a specified degree τ , it cannot be recovered in subsequent steps. The second part implies that if the i -th modular attribute transformation g_i induces larger changes in pixel space than g_j , then the corresponding attribute Z_i (typically a coarse-grained attribute) is lost at a later time step than Z_j (a fine-grained attribute). This theoretical result reveals that in the forward diffusion process, fine-grained attributes (e.g., texture) are lost earlier than coarse-grained ones (e.g., shape), with granularity measured by the magnitude of pixel-level changes induced by modifying the attribute.

This proposition also shows the overlapping area between domains is closely related to the DM’s inherent ambiguity in reconstructing degraded samples. Based on this insight, we reinterpret the overlapping area—created by predefined image degradation—as a domain-shared distribution. This serves as a valuable prior, enabling the network to extract domain-invariant representations.

3.3 DiDA Framework

Although intermediate domains generated via image degradation can facilitate cross-domain adaptation, they should contend with a wide range of degradation levels and alleviate the risk of semantic shift. To overcome these challenges, we propose DiDA with two key modules: **Degradation-based Intermediate Domain Construction** and **Semantic Shift Compensation**. Our framework processes images at varying degradation levels and disentangles semantic shift through a dedicated diffusion encoder and reconstruction head. Designed as a general and flexible solution, DiDA seamlessly integrates with existing network architectures and UDA methods.

Degradation-based Intermediate Domain Construction. Degradation operations, when applied incrementally from mild to severe, can gradually enlarge overlapping area between domain distributions and eliminate domain-specific attributes. To effectively capture domain-invariant information under such conditions, the encoder g should maintain stable and consistent feature representations across varying levels of degradation. We propose a general approach by formalizing continuous degradation operations as a diffusion forward process.

The learning objective of generative models can be framed as finding a transport map $\mathcal{T} : \mathbb{R}^d \rightarrow \mathbb{R}^d$ between two distributions, i.e., $X = \mathcal{T}(Z)$, where $X \sim \pi_x, Z \sim \pi_z$. Typically, Z follows a simple elementary (Gaussian) distribution for sampling to generate X from the data distribution π_x . In the diffusion process, the transport map is formulated as a Markov chain with learned Gaussian transitions starting at $X_T \sim \pi_z$:

$$X_T \rightarrow X_{T-1} \cdots X_t \xrightarrow{p_\theta(X_{t-1}|X_t)} X_{t-1} \cdots \rightarrow X_0, \quad (7)$$

which is termed as a reverse process in contrast to equation (4). In our case, $X_0 \sim \{\pi_s, \pi_t\}$ represents the distribution of the source or target domain, respectively. Since X_1, X_2, \dots, X_T can be viewed as latent codes of the same dimensionality as the data X_0 , we consider them as intermediate domains, which possess gradually increasing overlapping area compared to the original X_0 . This formulation enables a degradation-based domain bridging mechanism within the diffusion framework.

Semantic Shift Compensation. While degradation helps remove domain-specific cues, it also inevitably affects domain-invariant features. This degradation of essential semantic information hinders the encoder’s ability to extract discriminative representations, known as semantic shift. To address this challenge, we propose a compensation mechanism that effectively disentangles the semantic shift and aligns the extracted features with label semantics throughout the degradation process, enabling the network to process intermediate domains at any degradation level while maintaining semantic consistency.

In this module, a trainable diffusion encoder, g' , is introduced to map each degraded image x_t to the feature space \hat{Z} given t . This diffusion encoder g' is designed to capture the semantic shift information of the segmentation network’s encoder g when taking x_t as input. To this end, a time embedding module is added to specify the diffusion time t . It is implemented by the Transformer sinusoidal position embedding [84] to condition all blocks of g' on t . Then, the internal feature $z'_{(t,i)}$ in $block'_i$ is modulated with shift and bias:

$$\hat{z}_{(t,i)} = z'_{(t,i)}(MLP_s^i \circ Embed(t) + 1) + MLP_b^i \circ Embed(t), \quad (8)$$

which is operated at the channel dimension of $z'_{(t,i)}$. The resulting feature \hat{z}_t is required to compensate for the intermediate feature z_t from g to minimize the reconstruction error by being supervised with the loss L^R (see equation (6)), where f_θ is replaced by $\hat{f}_\theta = h' \circ (g + g')$. We perform feature fusion by adding hierarchical features through residual connections. Through this module, the network is empowered to precisely disentangle the degree of perturbation and align the extracted features with label semantics by compensating for the semantic shift. Meanwhile, it retains the capability to adapt domain-invariant knowledge to the original domain distribution.

To leverage intermediate domains for improved adaptation, we introduce a Degraded Image Consistency (DIC) loss:

$$\mathcal{L}^D = \sum_{i=1}^{N_S} \mathcal{L}_{ce}(\bar{f}_\theta(x_{i,t}^S, t), y_i^S, 1) + \sum_{i=1}^{N_T} \mathcal{L}_{ce}(\bar{f}_\theta(x_{i,t}^T, t), p_i^T, q^T), \quad (9)$$

where $\bar{f}_\theta = h \circ (g + g')$ and $x_{i,t}$ is degrade image of $x_{i,0}$, which can be obtained with equation (5). This loss enforces consistency between predictions on degraded and original images.

Training and Inference. The training pipeline is shown in Fig. 2 and detailed in Appendix A. The original operation in the self-training framework is fully retained, and DiDA can be considered as an additional plugin. In each training iteration, we conduct the forward process with a fixed noise schedule $\bar{\alpha}_t$ and random t sampled from a uniform distribution between 1 and T on the current training batch. Then, they are fed to the network $\bar{f}_\theta/\hat{f}_\theta$, which shares the same weights with student net f_θ , and diffusion time t is encoded through the time embedding module in diffusion encoder g' . The outputs of this step, prediction for segmentation map and noise, are individually supervised by DIC loss and reconstruction loss. The overall loss \mathcal{L} for DiDA is the weighted sum of the presented loss components:

$$\mathcal{L} = \mathcal{L}^S + \mathcal{L}^T + \lambda_D \mathcal{L}^D + \lambda_R \mathcal{L}^R. \quad (10)$$

During regular inference, only the backbone segmentation network $f_\theta = h \circ g$ is used, while the diffusion-specific components— g' and h' —are entirely removed. The input is an unprocessed image from X_0 , and there is no need to use the diffusion encoder or reconstruction head for noise prediction, meaning that no additional time consumption or network structure changes are required in this stage.

3.4 Expansion to Arbitrary Degradation

Diffusion models demonstrate flexibility in their choice of degradation operations beyond traditional Gaussian noise [2]. Building on this insight, we extend DiDA to support various degradation types while maintaining our core principles of intermediate domain construction and semantic shift perception. To demonstrate this generalization, we implement forward diffusion processes based

Table 1: Quantitative results of DiDA on different methods and benchmarks with CNN-based model (C) or Transformer-based model (T). * denotes the reproduced result.

Method	GTA. \rightarrow CS.		SYN. \rightarrow CS.		CS. \rightarrow ACDC	
	C	T	C	T	C	T
DAFormer [38]	56.0	68.3	54.7	60.9	55.4	
+DiDA	58.3 \uparrow 2.3	70.3 \uparrow 2.0	57.6 \uparrow 2.9	63.1 \uparrow 2.2	59.1 \uparrow 3.7	
HRDA [39]	63.0	73.8	61.2	65.8	68.0	
+DiDA	64.3 \uparrow 1.3	75.4 \uparrow 1.6	62.6 \uparrow 1.4	67.8 \uparrow 2.0	70.7 \uparrow 2.7	
MIC [40]	64.2	75.5*	62.4*	67.3	69.8*	
+DiDA	65.0 \uparrow 0.8	76.8\uparrow1.3	63.5 \uparrow 1.1	68.6\uparrow1.3	72.1\uparrow2.3	

Table 2: Component ablation analysis of DiDA built with DAFormer on GTA. \rightarrow CS.(val).

\mathcal{L}^D	\mathcal{L}^R	g_{time}	g'	h'	mIoU
-	-	-	-	-	68.3
✓	-	-	-	-	66.5
✓	-	✓	-	-	69.5
-	✓	-	-	✓	67.9
✓	✓	✓	-	-	69.4
-	-	-	✓	✓	69.9
✓	✓	-	✓	✓	70.3

on two fundamental vision tasks: deblurring and inpainting. These implementations preserve the network’s ability to perceive degradation levels and compensate for semantic shifts across different degradation operations. Please refer to Appendix B for details on the implementation.

4 Experiments

4.1 Implementation Details

Datasets. To comprehensively evaluate the performance of DiDA, we follow standard UDA protocols and conduct experiments on both synthetic-to-real and clear-to-adverse-weather adaptation scenarios. As synthetic datasets, we use GTAv [70] containing 24,966 images and SYNTHIA [71] with 9,400 images. For real-world datasets, we employ Cityscapes [21] with 2,975 training and 500 validation images representing clear weather conditions, and ACDC [72] containing 1,600 training, 406 validation, and 2,000 test images capturing adverse weather conditions (fog, night, rain, and snow). We report the intersection over union for each class as well as the mean IoU over all classes.

Base Segmentation Architectures and UDA Methods To demonstrate the versatility and adaptability of our method, we implement it on two widely-used network architectures and three progressively enhanced baseline methods. Specifically, we employ DeepLabV2 [5] with ResNet-101 [32] backbone and DAFormer [38] with MiT-B5 [90] backbone. Both of these network architectures have been pretrained on the ImageNet-1k [24] dataset. Building upon this foundation, we apply our framework to different methods in the DAFormer series, including DAFormer [38], HRDA [39], and MIC [40].

Training Details. We implement DiDA based on the MMSegmentation [20] framework. Depending on the complexity of the network architectures and UDA frameworks, all experiments are conducted on one or two RTX-3090 GPUs with 24 GB memory, with 40K training iterations and a batch size of 2. We train the network using the AdamW optimizer, with learning rates of 6×10^{-5} for the encoder and 6×10^{-4} for the decoder, a weight decay of 0.01, and a linear learning rate warm-up strategy for the first 1.5K iterations. The EMA coefficient for updating the teacher network is set to 0.999. We set $T = 100$ and use a sigmoid schedule [44] to obtain $\bar{\alpha}_t$. To achieve scale and quantity matching during feature fusion, we initialize a diffusion encoder h' with the same structure as the corresponding the segmentation encoder, along with extra time embedding modules. For the reconstruction head g' , we initialize an ASPP module [5] with a linear projector. For the reconstruction loss, the clean image x_0 or sampled noise ϵ is downsampled at a rate of $4\times$ or $8\times$ to match the input of the reconstruction head. We set DIC loss weight λ^D to 0.5, and reconstruction loss weight λ^R to 5 for DAFormer and 1 for DeepLabV2 to ensure a similar gradient magnitude induced by these different components. Finally, we report the mIoU using the last checkpoint of the student model f_θ without model selection.

4.2 Evaluation on Benchmark Datasets

Overall Quantitative Results. Tab. 1 shows quantitative results by building DiDA upon three mainstream methods with different architectures. We report results based on whole inference on DAFormer and slide inference on HRDA and MIC without any other test time augmentation strategies for a fair comparison. Whether with Transformer-based or CNN-based backbones, DiDA achieves consistent gains beyond all baselines, ranging from 0.8% to 3.7%. As expected, the performance improvement generally decreases when the baseline is stronger and closer to performance saturation. When implemented with DeepLabV2, the performance gain is slightly lower than DAFormer due to the coarse output ($8\times$ downsampling) for the optimization goal of reconstruction. It is worth noting that DiDA achieves new state-of-the-art performance when applied on MIC.

Table 3: UDA segmentation performance on GTA. \rightarrow CS., where the improvement by DiDA is marked as **bold**. The results are acquired with CNN-based model (C) in the first group or Transformer-based model (T) in the second group. * denotes the reproduced result.

Method	Arch.	Road	Sidewalk	Building	Wall	Fence	Pole	Light	Sign	Veg	Terrain	Sky	Person	Rider	Car	Truck	Bus	Train	Motor	Bike	mIoU
DACS [82]	C	89.9	39.7	87.9	39.7	39.5	38.5	46.4	52.8	88.0	44.0	88.8	67.2	35.8	84.5	45.7	50.2	0.2	27.3	34.0	52.1
I2F [61]	C	90.8	48.7	85.2	30.6	28.0	33.3	46.4	40.0	85.6	39.1	88.1	61.8	35.0	86.7	46.3	55.6	11.6	44.7	54.3	53.3
ProDA [98]	C	87.8	56.0	79.7	46.3	44.8	45.6	53.5	53.5	88.6	45.2	82.1	70.7	39.2	88.8	45.5	50.4	1.0	48.9	56.4	57.5
DAP [42]	C	94.5	63.1	89.1	29.8	47.5	50.4	56.7	58.7	89.5	50.2	87.0	73.6	38.6	91.3	50.2	52.9	0.0	50.2	63.5	59.8
CPSL [48]	C	92.3	59.5	84.9	45.7	29.7	52.8	61.5	59.5	87.9	41.6	85.0	73.0	35.5	90.4	48.7	73.9	26.3	53.8	53.9	60.8
MIC [40]	C	96.5	74.3	90.4	47.1	42.8	50.3	61.7	62.3	90.3	49.2	90.7	77.8	53.2	93.0	66.2	68.0	6.8	38.0	60.6	64.2
+DiDA	C	96.6	74.6	89.2	47.5	44.2	50.0	61.2	60.6	90.4	51.9	91.8	76.5	53.8	93.5	67.1	63.7	5.8	50.0	66.7	65.0
TransDA [10]	T	94.7	64.2	89.2	48.1	45.8	50.1	60.2	40.8	90.4	50.2	93.7	76.7	47.6	92.5	56.8	60.1	47.6	49.6	55.4	63.9
ADFormer [33]	T	96.7	75.1	88.8	57.5	45.9	45.6	55.4	59.8	90.2	45.6	92.1	70.8	43.0	91.0	78.9	79.3	68.7	52.7	65.0	69.2
CoPT [63]	T	97.6	80.9	91.6	62.1	55.9	59.3	66.7	70.5	91.9	53.0	94.4	80.0	55.6	94.7	87.1	88.6	82.1	65.0	68.8	76.1
DAFormer [38]	T	95.7	70.2	89.4	53.5	48.1	49.6	55.8	59.4	89.9	47.9	92.5	72.2	44.7	92.3	74.5	78.2	65.1	55.9	61.8	68.3
+FST [25]	T	95.3	67.7	89.3	55.5	47.1	50.1	57.2	58.6	89.9	51.0	92.9	72.7	46.3	92.5	78.0	81.6	74.4	57.7	62.6	69.3
+DiDA(B)	T	97.2	76.3	89.2	58.0	51.1	53.6	57.5	63.5	90.0	51.3	92.3	71.7	43.8	92.1	69.2	81.4	72.1	56.0	64.6	70.0
+DiDA(M)	T	96.4	75.3	90.5	57.6	49.2	53.4	58.6	64.4	90.5	52.6	92.5	71.8	40.8	92.6	70.6	81.7	66.1	57.6	64.0	69.8
+DiDA	T	96.9	74.7	88.9	54.4	49.8	53.5	57.5	63.9	90.6	50.4	92.2	71.5	50.8	92.2	76.1	82.1	70.7	53.2	66.8	70.3
HRDA [39]	T	96.4	74.4	91.0	61.6	51.5	57.1	63.9	69.3	91.3	48.4	94.2	79.0	52.9	93.9	84.1	85.7	75.9	63.9	67.5	73.8
+DiGA [75]	T	97.0	78.6	91.3	60.8	56.7	56.5	64.4	69.9	91.5	50.8	93.7	79.2	55.2	93.7	78.3	86.9	77.8	63.7	65.8	74.3
+DiDA	T	97.4	79.6	91.6	62.9	55.7	59.2	68.0	70.3	92.0	55.5	93.8	80.4	52.5	94.8	86.9	87.0	69.3	66.2	68.9	75.4
MIC* [40]	T	97.4	80.1	91.7	61.4	56.9	60.3	66.4	71.3	91.7	51.2	94.1	79.8	55.6	94.6	85.9	88.5	74.3	64.7	68.1	75.5
+DTS [43]	T	97.0	80.4	91.8	60.6	58.7	61.7	7.9	73.2	92.0	45.4	94.3	81.3	58.7	95.0	87.9	90.7	82.2	65.7	69.0	76.5
+DiDA	T	97.9	81.0	92.4	62.0	57.7	60.5	63.2	76.6	92.3	56.4	94.4	79.2	54.4	94.7	86.2	90.4	81.8	65.8	71.6	76.8

Class-level Comparison. We further display the class-wise performance on each benchmark in Tab. 3 and Tab. 4, with additional results provided in Tab. 5 (Appendix D), for detailed comparison. When combined with DiDA, most of classes achieve higher accuracy. We investigate that performance on *road*, *sidewalk*, *fence*, and *terrain* achieves consistent and relatively significant improvements over all UDA methods and datasets. These classes constitute the main scene and comprise abundant domain-specific texture information. By adding random Gaussian noise to images, these textures are broken while the context information is preserved, which is more robust over domains. Since DiDA establishes domain bridging through these progressively intensifying degraded images between domains, the network can focus more on domain-invariant context to enhance the adapting ability. Furthermore, we implement the extended version of DiDA on the DAFormer baseline with **Blur** and **Mask**, denoted as **B** and **M**, respectively. These extensions obtain less gain than the default version but show a certain potential if well-designed.

Comparison with other plug-in methods. We further compare DiDA with other plug-in approaches, such as FST [25], DiGA [75], and DTS [43]. Our method consistently demonstrates superior performance compared to these methods when built with the same baselines.

4.3 Diagnostic Experiments

Please refer to the Appendix D-L for further analysis, where we provide more experiment results, deeper ablation studies, and more visualization.

Component Ablation Analysis. To gain deeper insights, we analyze the proposed approach by ablating the components and evaluating the performance with DAFormer as the baseline on GTA \rightarrow CS. The results are presented in Tab. 2. The DiDA with complete components achieves a 2.0 mIoU gain on this baseline. To analyze the diffusion encoder and the module of time embedding respectively, we use the segmentation encoder g directly conditioned by time embedding as g_{time} without an extra diffusion encoder, as the baseline for ablation studies (row 6). We first ablate the module of time embedding, implying that the original network is equivalently trained with the randomly degraded images as additional data augmentation. The performance decreases heavily in this case (row 2) due to the excessive degradation of data, known as semantic shift problem. The introduced time embedding plays a vital role in encoding noise intensity information, indicating that we alleviate this issue by encoding time-specific semantic shift information. Then, we discard the loss terms, i.e., \mathcal{L}^D and \mathcal{L}^R , respectively (rows 3 and 4). Without \mathcal{L}^R , DiDA obtains less improvement, although it does not constrain segmentation results directly, indicating that \mathcal{L}^R helps to learn the module of time embedding and perceive the semantic shift. Discarding \mathcal{L}^D brings an accuracy drop since introducing \mathcal{L}^R only is inconsistent with the learning objective for high-level semantics. After that, the extra reconstruction head h' is ablated (row 5), which means that we obtain reconstruction results from the segmentation head h . It is also essential to avoid excessive disturbance for originally learned

Table 4: UDA segmentation performance on SYN. \rightarrow CS., where the improvement by DiDA is marked as **bold**. The results are acquired with CNN-based model (C) in the first group or Transformer-based model (T) in the second group.

Method	Arch.	Road	Sidewalk	Building	Wall	Fence	Pole	Light	Sign	Veg	Terrain	Sky	Person	Rider	Car	Truck	Bus	Train	Motor	Bike	mIoU
DACS [82]	C	80.6	25.1	81.9	21.5	2.9	37.2	22.7	24.0	83.7	-	90.8	67.6	38.3	82.9	-	38.9	-	28.5	47.6	48.3
I2F [61]	C	84.9	44.7	82.2	9.1	1.9	36.2	42.1	40.2	83.8	-	84.2	68.9	35.3	83.0	-	49.8	-	30.1	52.4	51.8
ProDA [98]	C	87.8	45.7	84.6	37.1	0.6	44.0	54.6	37.0	88.1	-	84.4	74.2	24.3	88.2	-	51.1	-	40.5	45.6	55.5
DAP [42]	C	84.2	46.5	82.5	35.1	0.2	46.7	53.6	45.7	89.3	-	87.5	75.7	34.6	91.7	-	73.5	-	49.4	60.5	59.8
CPSL [48]	C	87.2	43.9	85.5	33.6	0.3	47.7	57.4	37.2	87.8	-	88.5	79.0	32.0	90.6	-	49.4	-	50.8	59.8	57.9
TransDA [10]	T	90.4	54.8	86.4	31.1	1.7	53.8	61.1	37.1	90.3	-	93.0	71.2	25.3	92.3	-	66.0	-	44.4	49.8	59.3
ADFormer [33]	T	91.8	53.6	87.0	40.5	5.2	46.8	52.1	54.9	88.4	-	92.6	72.5	45.7	86.1	-	61.6	-	50.4	64.4	62.1
CoPT [63]	T	83.4	44.3	90.0	50.4	8.0	60.0	67.0	63.0	87.5	-	94.8	81.1	58.6	89.7	-	66.5	-	68.9	65.0	67.4
DAFormer [38]	T	84.5	40.7	88.4	41.5	6.5	50.0	55.0	54.6	86.0	-	89.8	73.2	48.2	87.2	-	53.2	-	53.9	61.7	60.9
+FST [25]	T	88.3	46.1	88.0	41.7	7.3	50.1	53.6	52.5	87.4	-	91.5	73.9	48.1	85.3	-	58.6	-	55.9	63.4	61.9
+DiDA	T	87.8	47.5	88.9	43.1	9.8	51.6	56.8	56.1	86.5	-	90.1	76.1	46.5	88.8	-	56.8	-	59.3	63.2	63.1
HRDA [39]	T	85.2	47.7	88.8	49.5	4.8	57.2	65.7	60.9	85.3	-	92.9	79.4	52.8	89.0	-	64.7	-	63.9	64.9	65.8
+DiGA [75]	T	88.5	49.9	90.1	51.4	6.6	55.3	64.8	62.7	88.2	-	93.5	78.6	51.8	89.5	-	62.2	-	61.0	65.8	66.2
+DiDA	T	87.9	52.9	89.6	54.3	11.6	56.6	63.8	61.2	87.6	-	94.1	79.9	54.2	90.5	-	71.5	-	67.1	62.3	67.8
MiC [40]	T	86.6	50.5	89.3	47.9	7.8	59.4	66.7	63.4	87.1	-	94.6	81.0	58.9	90.1	-	61.9	-	67.1	64.3	67.3
+DTS [43]	T	89.1	54.9	89.0	39.1	8.7	61.6	67.4	64.3	88.8	-	94.0	82.2	60.7	89.6	-	62.6	-	68.5	64.9	67.8
+DiDA	T	89.2	55.9	89.6	49.0	8.4	58.9	66.1	64.4	88.5	-	94.6	80.6	59.4	89.2	-	69.2	-	66.7	68.4	68.6

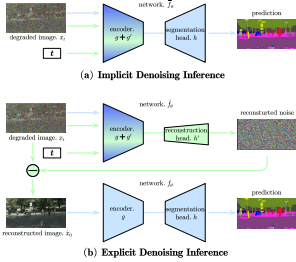


Figure 3: Demonstration of two modes of inference.

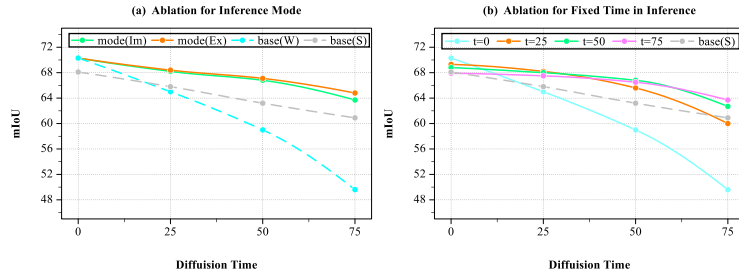


Figure 4: The performance variation with the degraded level.

features. In the end, the extra diffusion encoder is ablated (rows 6 and 7). Although g_{time} can perceive the semantic shift implicitly enabled by time embedding, it is more effective to introduce an extra diffusion encoder to compensate for the lost discriminative representation.

How DiDA Works. To further comprehend the working mechanism of DiDA, we design two modes for inference on degraded images with known diffusion time t , shown in Fig. 3. The first mode, called implicit denoising inference, is the same as what we used in the training phase of DiDA. The network \hat{f}_θ takes degraded images and t as inputs and generates segmentation results immediately. In contrast with this mode, the second mode segments the degraded images indirectly by predicting the noise through f_θ first for reconstruction and feeding them back to the network f_θ , which shares the same weight with \hat{f}_θ but no diffusion encoder, to obtain the final prediction. This mode is termed explicit denoising inference. We evaluate the performance difference between the two modes on different noise levels and construct two baselines for comparison. The strong baseline, called base(S), trains and inferences each model separately on intermediate domains with different noise levels. For the weak baseline, termed as base(W), we execute inference on these intermediate domains with f_θ . Fig. 4 (a) plots the performance curve throughout the diffusion forward process. The performance with implicit denoising inference is slightly lower than the explicit mode, and the gap between them is tiny. Both modes beat the strong baseline using a single network trained only once. It indicates that DiDA can perceive the semantic shift precisely and extract features in an implicit denoising manner during the training phase. Furthermore, unlike the explicit mode, the network \hat{f}_θ learns domain-invariant features directly from the degraded images to bridge the domain gap and heighten the adapting ability. These two factors jointly contribute to improving overall performance on UDA segmentation.

Inference with Fixed Diffusion Time. Based on the above discussion, we further evaluate the performance for inference with different fixed diffusion times t . The results are summarized in Fig. 4 (b). Note that $t = 0$ is equivalent to inference without the diffusion encoder, i.e., f_θ , which is the same as the weak baseline defined above. With the change of fixed diffusion time, there are two common properties among these curves: (i) the performance decreases along with the forward diffusion process, and (ii) at each fixed level of the forward process, inference with the same fixed

diffusion time t can achieve the current best precision, which is in accordance with the intuition. We can deduce that the higher t is fixed in the inference procedure, the flatter the corresponding performance curve will be. Although the optimal performance degrades, this phenomenon reveals a desirable property: inference with a fixed diffusion time t can enhance the network’s robustness against input perturbations, thereby improving its anti-interference capability.

5 Conclusions

In this paper, we propose DiDA, a degradation-based bridging framework for domain adaptive semantic segmentation. By simulating intermediate domains through simple image degradations and formalizing them as a diffusion process, DiDA effectively mitigates semantic shift and promotes domain-invariant feature learning. The framework is general and modular, supporting various degradation types and seamlessly integrating with diverse UDA methods and backbones. Extensive experiments demonstrate that DiDA consistently improves performance and achieves new state-of-the-art results on multiple standard UDA benchmarks.

Acknowledgements

This work was partially supported by the National Key R&D Program of China (Grant No. 2024YFB3909902), and the Youth Innovation Promotion Association of the Chinese Academy of Sciences (CAS).

References

- [1] Bai, Y., Yang, E., Wang, Z., Du, Y., Han, B., Deng, C., Wang, D., Liu, T.: Rsa: reducing semantic shift from aggressive augmentations for self-supervised learning. *Advances in Neural Information Processing Systems* **35**, 21128–21141 (2022)
- [2] Bansal, A., Borgnia, E., Chu, H.M., Li, J.S., Kazemi, H., Huang, F., Goldblum, M., Geiping, J., Goldstein, T.: Cold diffusion: Inverting arbitrary image transforms without noise. *arXiv preprint arXiv:2208.09392* (2022)
- [3] Baranchuk, D., Rubachev, I., Voynov, A., Khruikov, V., Babenko, A.: Label-efficient semantic segmentation with diffusion models. *arXiv preprint arXiv:2112.03126* (2021)
- [4] Bhojanapalli, S., Chakrabarti, A., Glasner, D., Li, D., Unterthiner, T., Veit, A.: Understanding robustness of transformers for image classification. In: *Proceedings of the IEEE/CVF international conference on computer vision*. pp. 10231–10241 (2021)
- [5] Chen, L.C., Papandreou, G., Kokkinos, I., Murphy, K., Yuille, A.L.: Deeplab: Semantic image segmentation with deep convolutional nets, atrous convolution, and fully connected crfs. *IEEE transactions on pattern analysis and machine intelligence* **40**(4), 834–848 (2017)
- [6] Chen, L.C., Papandreou, G., Schroff, F., Adam, H.: Rethinking atrous convolution for semantic image segmentation. *arXiv preprint arXiv:1706.05587* (2017)
- [7] Chen, L., Wei, Z., Jin, X., Chen, H., Zheng, M., Chen, K., Jin, Y.: Deliberated domain bridging for domain adaptive semantic segmentation. *Advances in Neural Information Processing Systems* **35**, 15105–15118 (2022)
- [8] Chen, M., Xue, H., Cai, D.: Domain adaptation for semantic segmentation with maximum squares loss. In: *Proceedings of the IEEE/CVF International Conference on Computer Vision*. pp. 2090–2099 (2019)
- [9] Chen, M., Zheng, Z., Yang, Y., Chua, T.S.: Pipa: Pixel-and patch-wise self-supervised learning for domain adaptative semantic segmentation. In: *Proceedings of the 31st ACM International Conference on Multimedia*. pp. 1905–1914 (2023)
- [10] Chen, R., Rong, Y., Guo, S., Han, J., Sun, F., Xu, T., Huang, W.: Smoothing matters: Momentum transformer for domain adaptive semantic segmentation. *arXiv preprint arXiv:2203.07988* (2022)

- [11] Chen, Y., Li, W., Sakaridis, C., Dai, D., Van Gool, L.: Domain adaptive faster r-cnn for object detection in the wild. In: Proceedings of the IEEE conference on computer vision and pattern recognition. pp. 3339–3348 (2018)
- [12] Chen, Y., Wang, H., Li, W., Sakaridis, C., Dai, D., Van Gool, L.: Scale-aware domain adaptive faster r-cnn. *International Journal of Computer Vision* **129**(7), 2223–2243 (2021)
- [13] Chen, Y., Li, W., Li, Z., Sun, R., Zhang, T., Xiong, Z., Wu, F.: Sam-glomeruli: Enhanced segment anything model for precise glomeruli segmentation. In: International Workshop on Medical Optical Imaging and Virtual Microscopy Image Analysis. pp. 182–191. Springer (2024)
- [14] Chen, Y., Sun, R., Li, W., Mai, H., Chen, S., Li, Z., Cheng, Z., Zhang, T.: Beyondmix: Leveraging structural priors and long-range dependencies for domain-invariant lidar segmentation. In: The Thirty-ninth Annual Conference on Neural Information Processing Systems (2025)
- [15] Chen, Y., Sun, R., Li, W., Mai, H., Luo, N., Pan, Y., Zhang, T.: Alleviate and mining: Rethinking unsupervised domain adaptation for mitochondria segmentation from pseudo-label perspective. In: Proceedings of the AAAI Conference on Artificial Intelligence. vol. 39, pp. 2339–2347 (2025)
- [16] Chen, Y.C., Lin, Y.Y., Yang, M.H., Huang, J.B.: Crdoco: Pixel-level domain transfer with cross-domain consistency. In: Proceedings of the IEEE/CVF conference on computer vision and pattern recognition. pp. 1791–1800 (2019)
- [17] Cheng, B., Misra, I., Schwing, A.G., Kirillov, A., Girdhar, R.: Masked-attention mask transformer for universal image segmentation. In: Proceedings of the IEEE/CVF conference on computer vision and pattern recognition. pp. 1290–1299 (2022)
- [18] Cheng, B., Schwing, A., Kirillov, A.: Per-pixel classification is not all you need for semantic segmentation. *Advances in Neural Information Processing Systems* **34**, 17864–17875 (2021)
- [19] Choi, J., Kim, T., Kim, C.: Self-ensembling with gan-based data augmentation for domain adaptation in semantic segmentation. In: Proceedings of the IEEE/CVF International Conference on Computer Vision. pp. 6830–6840 (2019)
- [20] Contributors, M.: Mmsegmentation: Openmmlab semantic segmentation toolbox and benchmark (2020)
- [21] Cordts, M., Omran, M., Ramos, S., Rehfeld, T., Enzweiler, M., Benenson, R., Franke, U., Roth, S., Schiele, B.: The cityscapes dataset for semantic urban scene understanding. In: Proceedings of the IEEE conference on computer vision and pattern recognition. pp. 3213–3223 (2016)
- [22] Cui, S., Wang, S., Zhuo, J., Su, C., Huang, Q., Tian, Q.: Gradually vanishing bridge for adversarial domain adaptation. In: Proceedings of the IEEE/CVF conference on computer vision and pattern recognition. pp. 12455–12464 (2020)
- [23] Dai, Y., Liu, J., Sun, Y., Tong, Z., Zhang, C., Duan, L.Y.: Idm: An intermediate domain module for domain adaptive person re-id. In: Proceedings of the IEEE/CVF International Conference on Computer Vision. pp. 11864–11874 (2021)
- [24] Deng, J., Dong, W., Socher, R., Li, L.J., Li, K., Fei-Fei, L.: Imagenet: A large-scale hierarchical image database. In: 2009 IEEE conference on computer vision and pattern recognition. pp. 248–255. Ieee (2009)
- [25] Du, Y., Shen, Y., Wang, H., Fei, J., Li, W., Wu, L., Zhao, R., Fu, Z., Liu, Q.: Learning from future: A novel self-training framework for semantic segmentation. *Advances in Neural Information Processing Systems* **35**, 4749–4761 (2022)
- [26] Du, Z., Li, J.: Diffusion-based probabilistic uncertainty estimation for active domain adaptation. *Advances in Neural Information Processing Systems* **36**, 17129–17155 (2023)
- [27] French, G., Oliver, A., Salimans, T.: Milking cowmask for semi-supervised image classification. arXiv preprint arXiv:2003.12022 (2020)

- [28] Ganin, Y., Ustinova, E., Ajakan, H., Germain, P., Larochelle, H., Laviolette, F., March, M., Lempitsky, V.: Domain-adversarial training of neural networks. *Journal of machine learning research* **17**(59), 1–35 (2016)
- [29] Ghifary, M., Kleijn, W.B., Zhang, M., Balduzzi, D., Li, W.: Deep reconstruction-classification networks for unsupervised domain adaptation. In: *Computer Vision–ECCV 2016: 14th European Conference, Amsterdam, The Netherlands, October 11–14, 2016, Proceedings, Part IV* 14. pp. 597–613. Springer (2016)
- [30] Gong, R., Li, W., Chen, Y., Gool, L.V.: Dlow: Domain flow for adaptation and generalization. In: *Proceedings of the IEEE/CVF conference on computer vision and pattern recognition*. pp. 2477–2486 (2019)
- [31] Goodfellow, I., Pouget-Abadie, J., Mirza, M., Xu, B., Warde-Farley, D., Ozair, S., Courville, A., Bengio, Y.: Generative adversarial nets. *Advances in neural information processing systems* **27** (2014)
- [32] He, K., Zhang, X., Ren, S., Sun, J.: Deep residual learning for image recognition. In: *Proceedings of the IEEE conference on computer vision and pattern recognition*. pp. 770–778 (2016)
- [33] He, L., Todorovic, S.: Attention decomposition for cross-domain semantic segmentation. In: *European Conference on Computer Vision*. pp. 414–431. Springer (2025)
- [34] He, W., Wang, Z., Zhang, Y.: Target semantics clustering via text representations for robust universal domain adaptation. In: *Proceedings of the AAAI Conference on Artificial Intelligence*. vol. 39, pp. 17132–17140 (2025)
- [35] He, W., Zhang, Y., Wang, Z.: Progressive distribution bridging: Unsupervised adaptation for large-scale pre-trained models via adaptive auxiliary data. In: *Proceedings of the IEEE/CVF international conference on computer vision* (2025)
- [36] Higgins, I., Amos, D., Pfau, D., Racaniere, S., Matthey, L., Rezende, D., Lerchner, A.: Towards a definition of disentangled representations. *arXiv preprint arXiv:1812.02230* (2018)
- [37] Ho, J., Jain, A., Abbeel, P.: Denoising diffusion probabilistic models. *Advances in neural information processing systems* **33**, 6840–6851 (2020)
- [38] Hoyer, L., Dai, D., Van Gool, L.: Daformer: Improving network architectures and training strategies for domain-adaptive semantic segmentation. In: *Proceedings of the IEEE/CVF Conference on Computer Vision and Pattern Recognition*. pp. 9924–9935 (2022)
- [39] Hoyer, L., Dai, D., Van Gool, L.: Hrda: Context-aware high-resolution domain-adaptive semantic segmentation. In: *European Conference on Computer Vision*. pp. 372–391. Springer (2022)
- [40] Hoyer, L., Dai, D., Wang, H., Van Gool, L.: Mic: Masked image consistency for context-enhanced domain adaptation. In: *Proceedings of the IEEE/CVF Conference on Computer Vision and Pattern Recognition*. pp. 11721–11732 (2023)
- [41] Huo, X., Xie, L., Hu, H., Zhou, W., Li, H., Tian, Q.: Domain-agnostic prior for transfer semantic segmentation. In: *Proceedings of the IEEE/CVF conference on Computer Vision and Pattern Recognition*. pp. 7075–7085 (2022)
- [42] Huo, X., Xie, L., Hu, H., Zhou, W., Li, H., Tian, Q.: Domain-agnostic priors for semantic segmentation under unsupervised domain adaptation and domain generalization. *International Journal of Computer Vision* pp. 1–23 (2024)
- [43] Huo, X., Xie, L., Zhou, W., Li, H., Tian, Q.: Focus on your target: A dual teacher-student framework for domain-adaptive semantic segmentation. *arXiv preprint arXiv:2303.09083* (2023)
- [44] Jabri, A., Fleet, D., Chen, T.: Scalable adaptive computation for iterative generation. *arXiv preprint arXiv:2212.11972* (2022)

- [45] Kingma, D.P., Welling, M.: Auto-encoding variational bayes. arXiv preprint arXiv:1312.6114 (2013)
- [46] Lee, S., Kim, N., Kim, S., Kwak, S.: Frest: Feature restoration for semantic segmentation under multiple adverse conditions. In: European Conference on Computer Vision. pp. 1–18. Springer (2024)
- [47] Li, D., Ling, H., Kim, S.W., Kreis, K., Fidler, S., Torralba, A.: Bigdatasetgan: Synthesizing imagenet with pixel-wise annotations. In: Proceedings of the IEEE/CVF Conference on Computer Vision and Pattern Recognition. pp. 21330–21340 (2022)
- [48] Li, R., Li, S., He, C., Zhang, Y., Jia, X., Zhang, L.: Class-balanced pixel-level self-labeling for domain adaptive semantic segmentation. In: Proceedings of the IEEE/CVF Conference on Computer Vision and Pattern Recognition. pp. 11593–11603 (2022)
- [49] Li, W., Sun, R., Li, Z., Zhang, T.: Towards robust pseudo-label learning in semantic segmentation: An encoding perspective. In: The Thirty-ninth Annual Conference on Neural Information Processing Systems (2025)
- [50] Li, W., Sun, R., Liao, B., Li, Z., Zhang, T.: Balanced learning for domain adaptive semantic segmentation. In: Forty-second International Conference on Machine Learning (2025)
- [51] Li, W., Liu, X., Yuan, Y.: Sigma: Semantic-complete graph matching for domain adaptive object detection. In: Proceedings of the IEEE/CVF Conference on Computer Vision and Pattern Recognition. pp. 5291–5300 (2022)
- [52] Li, Z., Li, W., Mai, H., Zhang, T., Xiong, Z.: Enhancing cell detection in histopathology images: a vit-based u-net approach. In: International Conference on Medical Image Computing and Computer-Assisted Intervention. pp. 150–160. Springer (2023)
- [53] Li, Z., Wang, Y., Li, W., Sun, R., Zhang, T.: Localization and expansion: A decoupled framework for point cloud few-shot semantic segmentation. In: European Conference on Computer Vision. pp. 18–34. Springer (2024)
- [54] Li, Z., Wang, Y., Li, W., Zhang, T., Liu, X.: Dual-agent optimization framework for cross-domain few-shot segmentation. In: Proceedings of the Computer Vision and Pattern Recognition Conference. pp. 9849–9859 (2025)
- [55] Li, Z., Wang, Y., Xiong, G., Li, W., Pan, Y., Zhang, T.: Generalized few-shot point cloud segmentation via llm-assisted hyper-relation matching. In: Proceedings of the IEEE/CVF international conference on computer vision (2025)
- [56] Long, J., Shelhamer, E., Darrell, T.: Fully convolutional networks for semantic segmentation. In: Proceedings of the IEEE conference on computer vision and pattern recognition. pp. 3431–3440 (2015)
- [57] Long, M., Cao, Y., Wang, J., Jordan, M.: Learning transferable features with deep adaptation networks. In: International conference on machine learning. pp. 97–105. PMLR (2015)
- [58] Lu, Z., Li, D., Song, Y.Z., Xiang, T., Hospedales, T.M.: Uncertainty-aware source-free domain adaptive semantic segmentation. *IEEE Transactions on Image Processing* (2023)
- [59] Luo, N., Wang, Y., Sun, R., Xiong, G., Zhang, T., Wu, F.: Exploring the better correlation for few-shot video object segmentation. *IEEE Transactions on Circuits and Systems for Video Technology* (2024)
- [60] Luo, X., Chen, W., Liang, Z., Yang, L., Wang, S., Li, C.: Crots: Cross-domain teacher–student learning for source-free domain adaptive semantic segmentation. *International Journal of Computer Vision* **132**(1), 20–39 (2024)
- [61] Ma, H., Lin, X., Yu, Y.: I2f: A unified image-to-feature approach for domain adaptive semantic segmentation. *IEEE Transactions on Pattern Analysis and Machine Intelligence* **46**(3), 1695–1710 (2024)

- [62] Mai, H., Sun, R., Zhang, T., Wu, F.: Rankmatch: Exploring the better consistency regularization for semi-supervised semantic segmentation. In: Proceedings of the IEEE/CVF Conference on Computer Vision and Pattern Recognition. pp. 3391–3401 (2024)
- [63] Mata, C., Ranasinghe, K., Ryoo, M.S.: Copt: Unsupervised domain adaptive segmentation using domain-agnostic text embeddings. In: European Conference on Computer Vision. pp. 424–440. Springer (2025)
- [64] Na, J., Jung, H., Chang, H.J., Hwang, W.: Fixbi: Bridging domain spaces for unsupervised domain adaptation. In: Proceedings of the IEEE/CVF conference on computer vision and pattern recognition. pp. 1094–1103 (2021)
- [65] Nichol, A.Q., Dhariwal, P.: Improved denoising diffusion probabilistic models. In: International Conference on Machine Learning. pp. 8162–8171. PMLR (2021)
- [66] Niemeijer, J., Schwonberg, M., Termöhlen, J.A., Schmidt, N.M., Fingscheidt, T.: Generalization by adaptation: Diffusion-based domain extension for domain-generalized semantic segmentation. In: Proceedings of the IEEE/CVF Winter Conference on Applications of Computer Vision. pp. 2830–2840 (2024)
- [67] Pan, Y., Sun, R., Li, W., Zhang, T.: Exploring weather-aware aggregation and adaptation for semantic segmentation under adverse conditions. In: Proceedings of the IEEE/CVF international conference on computer vision (2025)
- [68] Peng, D., Hu, P., Ke, Q., Liu, J.: Diffusion-based image translation with label guidance for domain adaptive semantic segmentation. In: Proceedings of the IEEE/CVF International Conference on Computer Vision. pp. 808–820 (2023)
- [69] Peng, D., Ke, Q., Ambikapathi, A., Yazici, Y., Lei, Y., Liu, J.: Unsupervised domain adaptation via domain-adaptive diffusion. *IEEE Transactions on Image Processing* (2024)
- [70] Richter, S.R., Vineet, V., Roth, S., Koltun, V.: Playing for data: Ground truth from computer games. In: Computer Vision—ECCV 2016: 14th European Conference, Amsterdam, The Netherlands, October 11–14, 2016, Proceedings, Part II 14. pp. 102–118. Springer (2016)
- [71] Ros, G., Sellart, L., Materzynska, J., Vazquez, D., Lopez, A.M.: The synthia dataset: A large collection of synthetic images for semantic segmentation of urban scenes. In: Proceedings of the IEEE conference on computer vision and pattern recognition. pp. 3234–3243 (2016)
- [72] Sakaridis, C., Dai, D., Van Gool, L.: Acdc: The adverse conditions dataset with correspondences for semantic driving scene understanding. In: Proceedings of the IEEE/CVF international conference on computer vision. pp. 10765–10775 (2021)
- [73] Salimans, T., Ho, J.: Progressive distillation for fast sampling of diffusion models. arXiv preprint arXiv:2202.00512 (2022)
- [74] Schölkopf, B., Locatello, F., Bauer, S., Ke, N.R., Kalchbrenner, N., Goyal, A., Bengio, Y.: Toward causal representation learning. *Proceedings of the IEEE* **109**(5), 612–634 (2021)
- [75] Shen, F., Gurram, A., Liu, Z., Wang, H., Knoll, A.: Diga: Distil to generalize and then adapt for domain adaptive semantic segmentation. In: Proceedings of the IEEE/CVF Conference on Computer Vision and Pattern Recognition. pp. 15866–15877 (2023)
- [76] Song, J., Meng, C., Ermon, S.: Denoising diffusion implicit models. arXiv preprint arXiv:2010.02502 (2020)
- [77] Su, X., Song, J., Meng, C., Ermon, S.: Dual diffusion implicit bridges for image-to-image translation. arXiv preprint arXiv:2203.08382 (2022)
- [78] Sun, R., Mai, H., Li, W., Chen, Y., Luo, N., Wang, Y., Zhang, T.: Beyond confidence: Exploiting homogeneous pattern for semi-supervised semantic segmentation. In: Forty-second International Conference on Machine Learning (2025)

- [79] Sun, R., Mai, H., Li, W., Chen, Y., Wang, Y.: Two losses, one goal: Aligning conflict gradients for semi-supervised semantic segmentation. In: Proceedings of the IEEE/CVF international conference on computer vision (2025)
- [80] Sun, R., Mai, H., Li, W., Zhang, T.: Towards unbiased learning in semi-supervised semantic segmentation. In: The Thirteenth International Conference on Learning Representations (2025)
- [81] Toldo, M., Michieli, U., Agresti, G., Zanuttigh, P.: Unsupervised domain adaptation for mobile semantic segmentation based on cycle consistency and feature alignment. *Image and Vision Computing* **95**, 103889 (2020)
- [82] Tranheden, W., Olsson, V., Pinto, J., Svensson, L.: Dacs: Domain adaptation via cross-domain mixed sampling. In: Proceedings of the IEEE/CVF Winter Conference on Applications of Computer Vision. pp. 1379–1389 (2021)
- [83] Tsai, Y.H., Hung, W.C., Schuler, S., Sohn, K., Yang, M.H., Chandraker, M.: Learning to adapt structured output space for semantic segmentation. In: Proceedings of the IEEE conference on computer vision and pattern recognition. pp. 7472–7481 (2018)
- [84] Vaswani, A., Shazeer, N., Parmar, N., Uszkoreit, J., Jones, L., Gomez, A.N., Kaiser, Ł., Polosukhin, I.: Attention is all you need. *Advances in neural information processing systems* **30** (2017)
- [85] Vu, T.H., Jain, H., Bucher, M., Cord, M., Pérez, P.: Advent: Adversarial entropy minimization for domain adaptation in semantic segmentation. In: Proceedings of the IEEE/CVF conference on computer vision and pattern recognition. pp. 2517–2526 (2019)
- [86] Wang, Y., Geng, Z., Jiang, F., Li, C., Wang, Y., Yang, J., Lin, Z.: Residual relaxation for multi-view representation learning. *Advances in Neural Information Processing Systems* **34**, 12104–12115 (2021)
- [87] Wang, Y., Sun, R., Luo, N., Pan, Y., Zhang, T.: Image-to-image matching via foundation models: A new perspective for open-vocabulary semantic segmentation. In: Proceedings of the IEEE/CVF Conference on Computer Vision and Pattern Recognition. pp. 3952–3963 (2024)
- [88] Wangkai, L., Zhaoyang, L., Rui, S., Huayu, M., Naisong, L., Wang, Y., Yuwen, P., Guoxin, X., Huakai, L., Zhiwei, X., et al.: Maunet: Modality-aware anti-ambiguity u-net for multi-modality cell segmentation. In: Competitions in Neural Information Processing Systems. pp. 1–12. PMLR (2023)
- [89] Wu, X., Wu, Z., Guo, H., Ju, L., Wang, S.: Dattet: A one-stage domain adaptation network for unsupervised nighttime semantic segmentation. In: Proceedings of the IEEE/CVF Conference on Computer Vision and Pattern Recognition. pp. 15769–15778 (2021)
- [90] Xie, E., Wang, W., Yu, Z., Anandkumar, A., Alvarez, J.M., Luo, P.: Segformer: Simple and efficient design for semantic segmentation with transformers. *Advances in Neural Information Processing Systems* **34**, 12077–12090 (2021)
- [91] Xu, J., Liu, S., Vahdat, A., Byeon, W., Wang, X., De Mello, S.: Open-vocabulary panoptic segmentation with text-to-image diffusion models. In: Proceedings of the IEEE/CVF Conference on Computer Vision and Pattern Recognition. pp. 2955–2966 (2023)
- [92] Xu, M., Zhang, J., Ni, B., Li, T., Wang, C., Tian, Q., Zhang, W.: Adversarial domain adaptation with domain mixup. In: Proceedings of the AAAI conference on artificial intelligence. vol. 34, pp. 6502–6509 (2020)
- [93] Yang, L., Qi, L., Feng, L., Zhang, W., Shi, Y.: Revisiting weak-to-strong consistency in semi-supervised semantic segmentation. In: Proceedings of the IEEE/CVF conference on computer vision and pattern recognition. pp. 7236–7246 (2023)
- [94] Yang, Y., Soatto, S.: Fda: Fourier domain adaptation for semantic segmentation. In: Proceedings of the IEEE/CVF conference on computer vision and pattern recognition. pp. 4085–4095 (2020)

- [95] Yue, Z., Wang, J., Sun, Q., Ji, L., Chang, E.I., Zhang, H., et al.: Exploring diffusion time-steps for unsupervised representation learning. arXiv preprint arXiv:2401.11430 (2024)
- [96] Yun, S., Han, D., Oh, S.J., Chun, S., Choe, J., Yoo, Y.: Cutmix: Regularization strategy to train strong classifiers with localizable features. In: Proceedings of the IEEE/CVF international conference on computer vision. pp. 6023–6032 (2019)
- [97] Zhang, H., Cisse, M., Dauphin, Y.N., Lopez-Paz, D.: mixup: Beyond empirical risk minimization. arXiv preprint arXiv:1710.09412 (2017)
- [98] Zhang, P., Zhang, B., Zhang, T., Chen, D., Wang, Y., Wen, F.: Prototypical pseudo label denoising and target structure learning for domain adaptive semantic segmentation. In: Proceedings of the IEEE/CVF conference on computer vision and pattern recognition. pp. 12414–12424 (2021)
- [99] Zhang, Y., Chen, S., Jiang, W., Zhang, Y., Lu, J., Kwok, J.T.: Domain-guided conditional diffusion model for unsupervised domain adaptation. *Neural Networks* **184**, 107031 (2025)
- [100] Zhang, Y., Ling, H., Gao, J., Yin, K., Lafleche, J.F., Barriuso, A., Torralba, A., Fidler, S.: Datasetgan: Efficient labeled data factory with minimal human effort. In: Proceedings of the IEEE/CVF Conference on Computer Vision and Pattern Recognition. pp. 10145–10155 (2021)
- [101] Zheng, Z., Yang, Y.: Rectifying pseudo label learning via uncertainty estimation for domain adaptive semantic segmentation. *International Journal of Computer Vision* **129**(4), 1106–1120 (2021)
- [102] Zhou, Q., Feng, Z., Gu, Q., Pang, J., Cheng, G., Lu, X., Shi, J., Ma, L.: Context-aware mixup for domain adaptive semantic segmentation. *IEEE Transactions on Circuits and Systems for Video Technology* **33**(2), 804–817 (2022)

NeurIPS Paper Checklist

1. Claims

Question: Do the main claims made in the abstract and introduction accurately reflect the paper's contributions and scope?

Answer: [Yes]

Justification: The abstract and introduction accurately reflect the main contributions. Please refer to abstract and Section 1.

Guidelines:

- The answer NA means that the abstract and introduction do not include the claims made in the paper.
- The abstract and/or introduction should clearly state the claims made, including the contributions made in the paper and important assumptions and limitations. A No or NA answer to this question will not be perceived well by the reviewers.
- The claims made should match theoretical and experimental results, and reflect how much the results can be expected to generalize to other settings.
- It is fine to include aspirational goals as motivation as long as it is clear that these goals are not attained by the paper.

2. Limitations

Question: Does the paper discuss the limitations of the work performed by the authors?

Answer: [Yes]

Justification: Please refer to Appendix N for our discussions on the limitations.

Guidelines:

- The answer NA means that the paper has no limitation while the answer No means that the paper has limitations, but those are not discussed in the paper.
- The authors are encouraged to create a separate "Limitations" section in their paper.
- The paper should point out any strong assumptions and how robust the results are to violations of these assumptions (e.g., independence assumptions, noiseless settings, model well-specification, asymptotic approximations only holding locally). The authors should reflect on how these assumptions might be violated in practice and what the implications would be.
- The authors should reflect on the scope of the claims made, e.g., if the approach was only tested on a few datasets or with a few runs. In general, empirical results often depend on implicit assumptions, which should be articulated.
- The authors should reflect on the factors that influence the performance of the approach. For example, a facial recognition algorithm may perform poorly when image resolution is low or images are taken in low lighting. Or a speech-to-text system might not be used reliably to provide closed captions for online lectures because it fails to handle technical jargon.
- The authors should discuss the computational efficiency of the proposed algorithms and how they scale with dataset size.
- If applicable, the authors should discuss possible limitations of their approach to address problems of privacy and fairness.
- While the authors might fear that complete honesty about limitations might be used by reviewers as grounds for rejection, a worse outcome might be that reviewers discover limitations that aren't acknowledged in the paper. The authors should use their best judgment and recognize that individual actions in favor of transparency play an important role in developing norms that preserve the integrity of the community. Reviewers will be specifically instructed to not penalize honesty concerning limitations.

3. Theory assumptions and proofs

Question: For each theoretical result, does the paper provide the full set of assumptions and a complete (and correct) proof?

Answer: [Yes]

Justification: Please refer to Section 3.2 for the complete proof and assumptions.

Guidelines:

- The answer NA means that the paper does not include theoretical results.
- All the theorems, formulas, and proofs in the paper should be numbered and cross-referenced.
- All assumptions should be clearly stated or referenced in the statement of any theorems.
- The proofs can either appear in the main paper or the supplemental material, but if they appear in the supplemental material, the authors are encouraged to provide a short proof sketch to provide intuition.
- Inversely, any informal proof provided in the core of the paper should be complemented by formal proofs provided in appendix or supplemental material.
- Theorems and Lemmas that the proof relies upon should be properly referenced.

4. Experimental result reproducibility

Question: Does the paper fully disclose all the information needed to reproduce the main experimental results of the paper to the extent that it affects the main claims and/or conclusions of the paper (regardless of whether the code and data are provided or not)?

Answer: [Yes]

Justification: We provide implementation details in Section 4 and Appendix A-C.

Guidelines:

- The answer NA means that the paper does not include experiments.
- If the paper includes experiments, a No answer to this question will not be perceived well by the reviewers: Making the paper reproducible is important, regardless of whether the code and data are provided or not.
- If the contribution is a dataset and/or model, the authors should describe the steps taken to make their results reproducible or verifiable.
- Depending on the contribution, reproducibility can be accomplished in various ways. For example, if the contribution is a novel architecture, describing the architecture fully might suffice, or if the contribution is a specific model and empirical evaluation, it may be necessary to either make it possible for others to replicate the model with the same dataset, or provide access to the model. In general, releasing code and data is often one good way to accomplish this, but reproducibility can also be provided via detailed instructions for how to replicate the results, access to a hosted model (e.g., in the case of a large language model), releasing of a model checkpoint, or other means that are appropriate to the research performed.
- While NeurIPS does not require releasing code, the conference does require all submissions to provide some reasonable avenue for reproducibility, which may depend on the nature of the contribution. For example
 - (a) If the contribution is primarily a new algorithm, the paper should make it clear how to reproduce that algorithm.
 - (b) If the contribution is primarily a new model architecture, the paper should describe the architecture clearly and fully.
 - (c) If the contribution is a new model (e.g., a large language model), then there should either be a way to access this model for reproducing the results or a way to reproduce the model (e.g., with an open-source dataset or instructions for how to construct the dataset).
 - (d) We recognize that reproducibility may be tricky in some cases, in which case authors are welcome to describe the particular way they provide for reproducibility. In the case of closed-source models, it may be that access to the model is limited in some way (e.g., to registered users), but it should be possible for other researchers to have some path to reproducing or verifying the results.

5. Open access to data and code

Question: Does the paper provide open access to the data and code, with sufficient instructions to faithfully reproduce the main experimental results, as described in supplemental material?

Answer: [No]

Justification: The code will be open-sourced to the community upon acceptance of the paper.

Guidelines:

- The answer NA means that paper does not include experiments requiring code.
- Please see the NeurIPS code and data submission guidelines (<https://nips.cc/public/guides/CodeSubmissionPolicy>) for more details.
- While we encourage the release of code and data, we understand that this might not be possible, so “No” is an acceptable answer. Papers cannot be rejected simply for not including code, unless this is central to the contribution (e.g., for a new open-source benchmark).
- The instructions should contain the exact command and environment needed to run to reproduce the results. See the NeurIPS code and data submission guidelines (<https://nips.cc/public/guides/CodeSubmissionPolicy>) for more details.
- The authors should provide instructions on data access and preparation, including how to access the raw data, preprocessed data, intermediate data, and generated data, etc.
- The authors should provide scripts to reproduce all experimental results for the new proposed method and baselines. If only a subset of experiments are reproducible, they should state which ones are omitted from the script and why.
- At submission time, to preserve anonymity, the authors should release anonymized versions (if applicable).
- Providing as much information as possible in supplemental material (appended to the paper) is recommended, but including URLs to data and code is permitted.

6. Experimental setting/details

Question: Does the paper specify all the training and test details (e.g., data splits, hyper-parameters, how they were chosen, type of optimizer, etc.) necessary to understand the results?

Answer: [Yes]

Justification: Please refer to Section 4 and Appendix D-L for experimental details.

Guidelines:

- The answer NA means that the paper does not include experiments.
- The experimental setting should be presented in the core of the paper to a level of detail that is necessary to appreciate the results and make sense of them.
- The full details can be provided either with the code, in appendix, or as supplemental material.

7. Experiment statistical significance

Question: Does the paper report error bars suitably and correctly defined or other appropriate information about the statistical significance of the experiments?

Answer: [No]

Justification: Error bars are not reported because it would be too computationally expensive.

Guidelines:

- The answer NA means that the paper does not include experiments.
- The authors should answer "Yes" if the results are accompanied by error bars, confidence intervals, or statistical significance tests, at least for the experiments that support the main claims of the paper.
- The factors of variability that the error bars are capturing should be clearly stated (for example, train/test split, initialization, random drawing of some parameter, or overall run with given experimental conditions).
- The method for calculating the error bars should be explained (closed form formula, call to a library function, bootstrap, etc.)
- The assumptions made should be given (e.g., Normally distributed errors).
- It should be clear whether the error bar is the standard deviation or the standard error of the mean.

- It is OK to report 1-sigma error bars, but one should state it. The authors should preferably report a 2-sigma error bar than state that they have a 96% CI, if the hypothesis of Normality of errors is not verified.
- For asymmetric distributions, the authors should be careful not to show in tables or figures symmetric error bars that would yield results that are out of range (e.g. negative error rates).
- If error bars are reported in tables or plots, The authors should explain in the text how they were calculated and reference the corresponding figures or tables in the text.

8. Experiments compute resources

Question: For each experiment, does the paper provide sufficient information on the computer resources (type of compute workers, memory, time of execution) needed to reproduce the experiments?

Answer: [Yes]

Justification: We describe the computer resources in Section 4 and Appendix E.

Guidelines:

- The answer NA means that the paper does not include experiments.
- The paper should indicate the type of compute workers CPU or GPU, internal cluster, or cloud provider, including relevant memory and storage.
- The paper should provide the amount of compute required for each of the individual experimental runs as well as estimate the total compute.
- The paper should disclose whether the full research project required more compute than the experiments reported in the paper (e.g., preliminary or failed experiments that didn't make it into the paper).

9. Code of ethics

Question: Does the research conducted in the paper conform, in every respect, with the NeurIPS Code of Ethics <https://neurips.cc/public/EthicsGuidelines>?

Answer: [Yes]

Justification: The research conducted in this paper adheres fully to the NeurIPS Code of Ethics.

Guidelines:

- The answer NA means that the authors have not reviewed the NeurIPS Code of Ethics.
- If the authors answer No, they should explain the special circumstances that require a deviation from the Code of Ethics.
- The authors should make sure to preserve anonymity (e.g., if there is a special consideration due to laws or regulations in their jurisdiction).

10. Broader impacts

Question: Does the paper discuss both potential positive societal impacts and negative societal impacts of the work performed?

Answer: [Yes]

Justification: Please refer to Appendix N for our discussions on the societal impacts.

Guidelines:

- The answer NA means that there is no societal impact of the work performed.
- If the authors answer NA or No, they should explain why their work has no societal impact or why the paper does not address societal impact.
- Examples of negative societal impacts include potential malicious or unintended uses (e.g., disinformation, generating fake profiles, surveillance), fairness considerations (e.g., deployment of technologies that could make decisions that unfairly impact specific groups), privacy considerations, and security considerations.

- The conference expects that many papers will be foundational research and not tied to particular applications, let alone deployments. However, if there is a direct path to any negative applications, the authors should point it out. For example, it is legitimate to point out that an improvement in the quality of generative models could be used to generate deepfakes for disinformation. On the other hand, it is not needed to point out that a generic algorithm for optimizing neural networks could enable people to train models that generate Deepfakes faster.
- The authors should consider possible harms that could arise when the technology is being used as intended and functioning correctly, harms that could arise when the technology is being used as intended but gives incorrect results, and harms following from (intentional or unintentional) misuse of the technology.
- If there are negative societal impacts, the authors could also discuss possible mitigation strategies (e.g., gated release of models, providing defenses in addition to attacks, mechanisms for monitoring misuse, mechanisms to monitor how a system learns from feedback over time, improving the efficiency and accessibility of ML).

11. Safeguards

Question: Does the paper describe safeguards that have been put in place for responsible release of data or models that have a high risk for misuse (e.g., pretrained language models, image generators, or scraped datasets)?

Answer: [No]

Justification: The paper poses no such risks.

Guidelines:

- The answer NA means that the paper poses no such risks.
- Released models that have a high risk for misuse or dual-use should be released with necessary safeguards to allow for controlled use of the model, for example by requiring that users adhere to usage guidelines or restrictions to access the model or implementing safety filters.
- Datasets that have been scraped from the Internet could pose safety risks. The authors should describe how they avoided releasing unsafe images.
- We recognize that providing effective safeguards is challenging, and many papers do not require this, but we encourage authors to take this into account and make a best faith effort.

12. Licenses for existing assets

Question: Are the creators or original owners of assets (e.g., code, data, models), used in the paper, properly credited and are the license and terms of use explicitly mentioned and properly respected?

Answer: [Yes]

Justification: All models and baselines from existing assets are properly cited.

Guidelines:

- The answer NA means that the paper does not use existing assets.
- The authors should cite the original paper that produced the code package or dataset.
- The authors should state which version of the asset is used and, if possible, include a URL.
- The name of the license (e.g., CC-BY 4.0) should be included for each asset.
- For scraped data from a particular source (e.g., website), the copyright and terms of service of that source should be provided.
- If assets are released, the license, copyright information, and terms of use in the package should be provided. For popular datasets, paperswithcode.com/datasets has curated licenses for some datasets. Their licensing guide can help determine the license of a dataset.
- For existing datasets that are re-packaged, both the original license and the license of the derived asset (if it has changed) should be provided.

- If this information is not available online, the authors are encouraged to reach out to the asset’s creators.

13. **New assets**

Question: Are new assets introduced in the paper well documented and is the documentation provided alongside the assets?

Answer: [NA]

Justification: The paper does not release new assets.

Guidelines:

- The answer NA means that the paper does not release new assets.
- Researchers should communicate the details of the dataset/code/model as part of their submissions via structured templates. This includes details about training, license, limitations, etc.
- The paper should discuss whether and how consent was obtained from people whose asset is used.
- At submission time, remember to anonymize your assets (if applicable). You can either create an anonymized URL or include an anonymized zip file.

14. **Crowdsourcing and research with human subjects**

Question: For crowdsourcing experiments and research with human subjects, does the paper include the full text of instructions given to participants and screenshots, if applicable, as well as details about compensation (if any)?

Answer: [NA]

Justification: The paper does not involve crowdsourcing nor research with human subjects.

Guidelines:

- The answer NA means that the paper does not involve crowdsourcing nor research with human subjects.
- Including this information in the supplemental material is fine, but if the main contribution of the paper involves human subjects, then as much detail as possible should be included in the main paper.
- According to the NeurIPS Code of Ethics, workers involved in data collection, curation, or other labor should be paid at least the minimum wage in the country of the data collector.

15. **Institutional review board (IRB) approvals or equivalent for research with human subjects**

Question: Does the paper describe potential risks incurred by study participants, whether such risks were disclosed to the subjects, and whether Institutional Review Board (IRB) approvals (or an equivalent approval/review based on the requirements of your country or institution) were obtained?

Answer: [NA]

Justification: The paper does not involve crowdsourcing nor research with human subjects

Guidelines:

- The answer NA means that the paper does not involve crowdsourcing nor research with human subjects.
- Depending on the country in which research is conducted, IRB approval (or equivalent) may be required for any human subjects research. If you obtained IRB approval, you should clearly state this in the paper.
- We recognize that the procedures for this may vary significantly between institutions and locations, and we expect authors to adhere to the NeurIPS Code of Ethics and the guidelines for their institution.
- For initial submissions, do not include any information that would break anonymity (if applicable), such as the institution conducting the review.

16. **Declaration of LLM usage**

Question: Does the paper describe the usage of LLMs if it is an important, original, or non-standard component of the core methods in this research? Note that if the LLM is used only for writing, editing, or formatting purposes and does not impact the core methodology, scientific rigorousness, or originality of the research, declaration is not required.

Answer: [NA]

Justification: LLM is used only for editing.

Guidelines:

- The answer NA means that the core method development in this research does not involve LLMs as any important, original, or non-standard components.
- Please refer to our LLM policy (<https://neurips.cc/Conferences/2025/LLM>) for what should or should not be described.

A Implementation Details of DiDA

In this section, we provide the pseudo algorithms to explain implementation details of DiDA, as shown in Alg. 1. Our method is designed as a plug-and-play module applicable to any self-training-based UDA framework, introducing no additional computational overhead during inference.

Algorithm 1 Pseudo algorithms of DiDA.

```

1: Inputs: Source Domain  $D_s = (x_i^S, y_i^S)_{i=1}^{N_s}$ , Target Domain  $D_t = (x_i^T)_{i=1}^{N_T}$ 
2: Define: Student Network  $f_\theta$ , Teacher Network  $f_\phi$ , Diffusion Encoder  $g'$ , Reconstruction Head  $h'$ , Noise Schedule  $\bar{\alpha}_t$ , Diffusion Steps  $T$ , Momentum Coefficient  $\beta$ 
3: Output: Student Network  $f_\theta$ 
4: for each batch of  $(x_i^S, y_i^S), x_i^T$  in  $D_s, D_t$  do
5:   # Source Domain:
6:   Calculate  $\mathcal{L}^S$  for  $f_\theta$  by Eq. (1) ▷ Supervised loss
7:   # Target Domain:
8:   Obtain pseudo-labels from  $f_\phi$  by Eq. (3)
9:   Calculate  $\mathcal{L}^T$  for  $f_\theta$  by Eq. (4) ▷ Adaptation loss
10:  # Degradation-based Intermediate Domain Construction:
11:  Sample  $t \sim \text{Uniform}(1, T)$ 
12:  Obtain degraded images  $x_{i,t}^S, x_{i,t}^T$  by Eq. (6)
13:  # Semantic Shift Compensation:
14:  Calculate  $\mathcal{L}^D$  for  $\hat{f}_\theta = h \circ (g + g')$  by Eq. (10) ▷ Degraded image consistency loss
15:  Calculate  $\mathcal{L}^R$  for  $\hat{f}_\theta = h' \circ (g + g')$  by Eq. (7) ▷ Reconstruction loss
16:  # Training:
17:  Gradient backward  $\mathcal{L}^S + \mathcal{L}^T + \lambda_D \mathcal{L}^D + \lambda_R \mathcal{L}^R$  ▷ Update student model
18:  # EMA Update:
19:   $\phi \leftarrow \beta \phi + (1 - \beta) \theta$  ▷ Update teacher model
20: end for

```

B Details in Expansion Versions

In this section, we describe the details of our implementation for expansion versions of DiDA, in which we replace the degradation operation in the diffusion forward process with **blur** and **mask**.

Image Blur. Given the Gaussian kernels $\{G_s\}$, the forward process can be simply defined as:

$$x_t = G_t * x_{t-1} = G_t * \dots * G_1 * x_0 = \bar{G}_t * x_0, \quad (11)$$

where $*$ represents the convolution operator to apply the Gaussian blur operation on the image. Then, the model \hat{f}_θ is trained for deblurring to invert this blurred diffusion process.

Following the setting of cold diffusion [2], we define T Gaussian kernels: G_1, \dots, G_T to execute gradual blurring. For instance, we set $T = 100$ with a Gaussian kernel of 31×31 , and the standard deviation of the Gaussian kernel grows exponentially with time t at the rate of 0.02.

Image Mask. To implement the incremental mask operation on the image with the diffusion time steps, we define this process with cowmask [27]. With the schedule $\bar{\alpha}_t$ as a threshold, we can generate the cowmask \mathcal{M}_t and obtain x_t by element-wise multiplication of the mask and image:

$$x_t = \mathcal{M}_t \odot x_0, \quad (12)$$

and the inpainting model is trained to restore the image. The procedure for generating a masked image with cowmask and τ is provided in Algorithm 2, and we set the std $\delta = 6$.

To extend our method with the above-defined forward process, we only need to replace the degraded image sampling operation and modify the reconstruction loss to predict the clean image x_0 directly:

$$\mathcal{L}^R = \lambda_t \|\hat{f}_\theta(x_t, t) - x_0\|_2^2, \quad (13)$$

where λ_t is a t -dependent loss weight, defined as a fixed value computed from the noise schedule $\{\alpha_t\}_{t=1}^T$ [73], introduced to balance the contribution of different degradation levels.

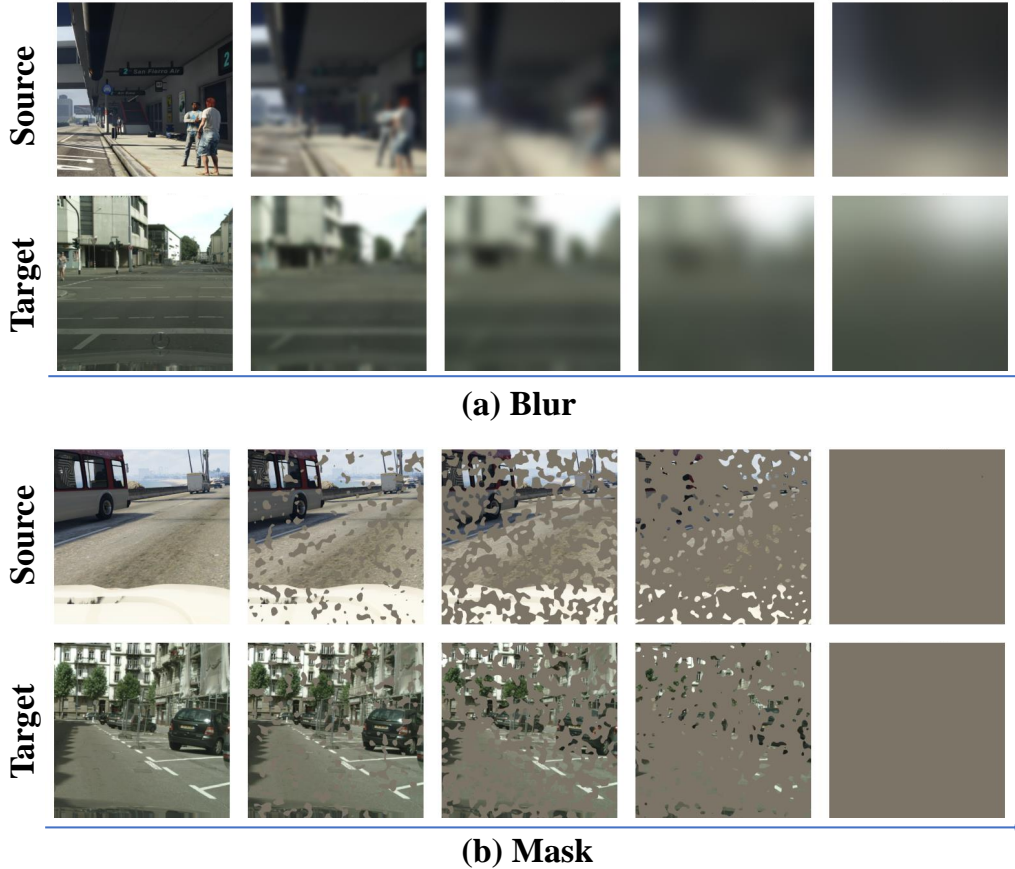


Figure 5: The examples that extend DiDA to any other forward diffusion process defined by arbitrary image degradation operations. (a) shows image blurred process and (b) shows image masked process.

Algorithm 2 CowMask generation algorithm with the threshold $\tau \in [0, 1]$ as the ratio.

Require: original image x^O , threshold τ , std δ

Ensure: masked image x^M

- 1: sample Gaussian noise $\epsilon \sim \mathcal{N}(0, \mathbf{I})$
 - 2: filter noise $\epsilon_f = \text{gaussian_filter_2d}(\epsilon, \delta)$
 - 3: compute mean $m = \text{mean}(\epsilon_f)$
 - 4: compute std_dev $s = \text{std_dev}(\epsilon_f)$
 - 5: compute noise threshold $p = m + \sqrt{2}erf^{-1}(2\tau - 1)s$
 - 6: threshold filtered noise $\mathcal{M} = \epsilon_f < p$
 - 7: mask image $x^M = x^O \odot \mathcal{M}$
 - 8: **return** x^M
-

C Architecture of Time Embedding Module

In this section, we illustrate the details of the time embedding module introduced in different backbones. As shown in Fig. 6, we condition all blocks of models on t , whether Transformer-based architecture or CNN-based architecture. The diffusion time t is first encoded by Transformer sinusoidal position embedding [84] and projected to time embedding through 2 layers MLP. Then, the time embedding is encoded by MLP_s^i and MLP_b^i to obtain shift and bias and ensure the same channel dimension as the corresponding feature. In the end, each block’s internal feature f_i is modulated through multiplication and addition operations at the channel dimension.

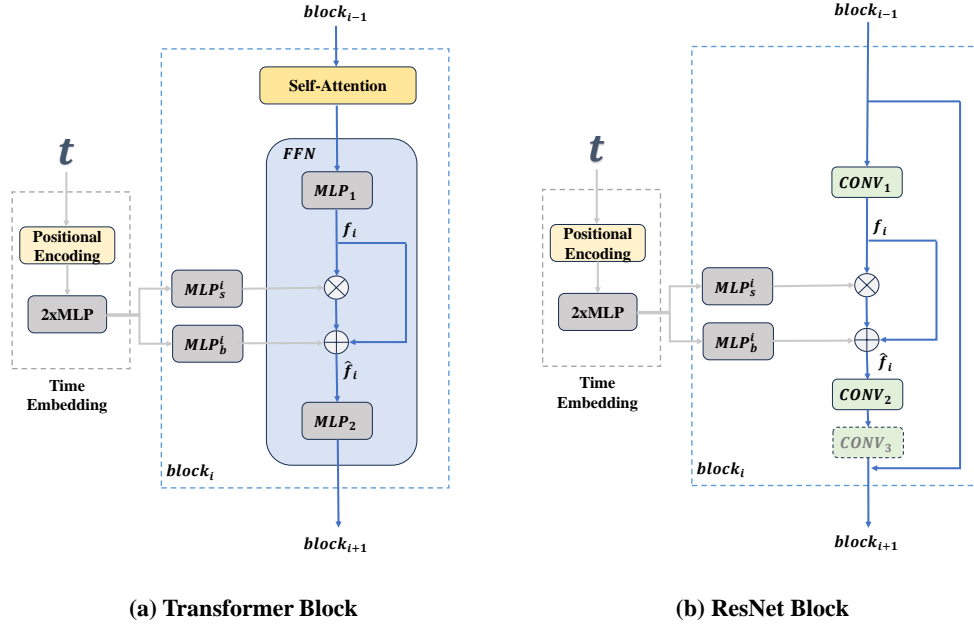


Figure 6: Architecture of time embedding module in different backbones.

Table 5: UDA segmentation performance on CS. \rightarrow ACDC, where the improvement by DiDA is marked as **bold**. The results are acquired with CNN-based model (C) in the first group or Transformer-based model (T) in the second group. * denotes the reproduced result.

Method	Arch.	Road	Sidewalk	Building	Wall	Fence	Pole	Light	Sign	Veg	Terrain	Sky	Person	Rider	Car	Truck	Bus	Train	Motor	Bike	mIoU
ADVENT [85]	C	72.9	14.3	40.5	16.6	21.2	9.3	17.4	21.2	63.8	23.8	18.3	32.6	19.5	69.5	36.2	34.5	46.2	26.9	36.1	32.7
DANNet [89]	C	84.3	54.2	77.6	38.0	30.0	18.9	41.6	35.2	71.3	39.4	86.6	48.7	29.2	76.2	41.6	43.0	58.6	32.6	43.9	50.0
FREST [46]	T	93.3	72.2	88.3	52.4	46.6	58.6	66.2	66.1	86.1	58.6	95.3	69.9	49.2	89.1	75.1	79.4	83.0	52.9	61.4	70.7
DAFormer [38]	T	58.4	51.3	84.0	42.7	35.1	50.7	30.0	57.0	74.8	52.8	51.3	58.3	32.6	82.7	58.3	54.9	82.4	44.1	50.7	55.4
+DiDA	T	68.5	52.5	82.5	43.4	42.7	59.8	60.3	53.4	75.7	40.2	63.7	59.3	30.4	87.3	68.6	76.1	79.5	41.9	36.6	59.1
HRDA [39]	T	88.3	57.9	88.1	55.2	36.7	56.3	62.9	65.3	74.2	57.7	85.9	68.8	45.7	88.5	76.4	82.4	87.7	52.7	60.4	68.0
+DiDA	T	90.7	65.4	89.3	58.3	50.1	68.7	70.8	66.6	79.1	46.2	67.1	73.0	49.4	85.2	85.9	89.4	91.5	56.3	60.1	70.7
MIC* [40]	T	90.1	65.0	87.7	55.5	43.3	60.6	63.8	66.2	75.8	54.3	85.0	69.5	47.4	88.6	80.7	89.5	88.8	55.4	59.1	69.8
+DiDA	T	90.5	68.6	89.0	62.9	50.1	65.4	66.3	68.8	75.6	51.9	84.3	70.0	51.4	88.1	82.4	92.5	92.2	56.6	63.6	72.1

D Additional Experiment Results

In this section, we evaluate the performance of our method on the CS. \rightarrow ACDC adaptation task, which involves large domain shifts caused by adverse weather conditions such as rain, snow, and nighttime. As shown in Tab. 5, DiDA consistently improves the performance of multiple baseline models, including DAFormer, HRDA, and MIC, with a gain ranging from 2.3% to 3.7% mIoU. These improvements are highlighted in bold.

We attribute DiDA’s superior performance in this scenario to the similarity between image degradation operations and real-world image corruptions caused by bad weather. Notably, the improvements are especially significant in classes that are typically affected by weather degradation, such as *traffic light*, *sign*, and *pole*. The degradation-aware training in DiDA (e.g., blur, noise, contrast reduction) helps the model learn more robust and generalizable features that align well with the characteristics of the ACDC dataset. In other words, DiDA implicitly narrows the domain gap by simulating weather-induced artifacts during training.

E DiDA Efficiency Analysis

In this section, we analyze the computational overhead introduced by DiDA in terms of GPU memory usage, iteration time, and total training time. As summarized in Table 6, while DiDA brings consistent

performance improvements across various UDA baselines, it also introduces moderate increases in computational cost.

Specifically, DiDA increases the GPU memory usage by approximately 60–70%, while it is computationally efficient, with an increase of 0.3-0.5s per iteration for each method. This overhead mainly stems from the additional modules introduced by DiDA, as illustrated in Algorithm 1. These include: (1) the diffusion-based degradation encoder g' , used to handle intermediate degraded domains; (2) the reconstruction head h' , which enforces semantic consistency via reconstruction and consistency losses (\mathcal{L}^D , \mathcal{L}^R); (3) additional forward passes on degraded inputs for both source and target domains. Despite this increase in resource usage, DiDA’s design is modular and parallelizable, and the degradation-based learning can be seamlessly integrated with existing teacher–student frameworks. We argue that the trade-off is justified, as the performance boosts brought by DiDA (up to +3.7% mIoU) outweigh the moderate increase in training cost, especially in challenging real-world adaptation scenarios like CS.→ACDC.

To further enhance the efficiency of our method, we additionally provide a memory-friendly variant, denoted as DiDA (g_{time}). As shown in row 6 of Table 2, this version avoids the explicit use of the diffusion encoder, and instead implicitly models the t -specific semantic shift through a lightweight time embedding. Despite its simplified design, DiDA (g_{time}) still achieves a comparable performance gain when compared to the full version (row 6 vs. row 7). By eliminating the diffusion encoder, DiDA (g_{time}) significantly reduces GPU memory consumption—saving up to 15–20% compared to the full version—while also slightly accelerating the training process. This makes it a practical trade-off option for scenarios with limited hardware resources.

Furthermore, DiDA is only applied during the training phase. No architectural modifications or additional computations are introduced at inference time, ensuring that the inference speed and resource consumption remain identical to the baseline models.

Table 6: Computational resource requirements comparison

Methods	GPU Memory (MB)	Time per iter (s)	Total Time (h)
DAFormer [38]	9,807	1.32	14.5 (40K iters)
+DiDA (g_{time})	12754	1.59	17.8 (40K iters)
+DiDA	15856	1.64	18.5 (40K iters)
HRDA [39]	22325	2.11	23.5 (40K iters)
+DiDA (g_{time})	16727×2	2.58	28.7 (40K iters)
+DiDA	19337×2	2.64	29.4 (40K iters)
MIC [40]	22370	2.60	28.9 (40K iters)
+DiDA (g_{time})	16813 ×2	3.03	33.7 (40K iters)
+DiDA	19343 ×2	3.13	34.8 (40K iters)

F Influence of Parameter Settings

In this section, we further study the influence of parameter settings introduced in DiDA, i.e., DIC loss weight λ_D , reconstruction loss weight λ_R , and diffusion steps T . All experiments are conducted with DAFormer [38] on GTA→CS.

DIC Loss Weight λ_D . We first study the weight of the DIC loss λ_D in Tab. 7. The weight for the DIC loss is sensitive to the UDA performance. Reducing the weight progressively diminishes performance until no DIC is used. A larger weight also results in decreased performance. If the weight is too large, such as $\lambda_D = 5$, it can lead to a significant decline in performance due to excessive disturbance.

Reconstruction Loss Weight λ_R . The weight of the reconstruction loss is also studied in a similar way (see Tab. 8). Based on the analysis above, we can draw a similar conclusion, with the difference being that this loss item has a slightly diminished impact compared to the previous one. The results demonstrate that values ranging from 1 to 10 consistently yield good UDA performance, providing a reasonably wide range for selecting robust hyperparameters.

Diffusion Steps T . We also study the value selection of diffusion steps T (see Tab. 9). Notice that too large a value, like $T = 1000$, does not result in optimal performance, which is the default setting for DDPM [37] to facilitate high-quality generation. In the UDA setting, the number of iterations

and batch size is far less than the requirement to train the generative model. Therefore, we make adjustments to reduce the diffusion steps T , ensuring they are more suitable for this task. In our experiments, a value around 100 can achieve consistently good performance.

Table 7: Parameter study of loss weight λ_D .

Weight λ_D	0	0.1	0.25	0.5	1	5
mIoU	67.9	69.6	70.1	70.3	69.8	64.1

Table 9: Parameter study of diffusion steps T .

Diffusion Steps T	10	50	100	200	1000
mIoU	69.3	70.2	70.3	70.0	70.1

Table 11: Results on GTA. \rightarrow CS built with extended versions.

Method	base	B	M
DAFormer [38]	68.3	70.0	69.8
HRDA [39]	73.8	75.3	74.9
MIC [40]	75.9	76.7	76.6

Table 8: Parameter study of loss weight λ_R .

Weight λ_R	0	1	2.5	5	10	50
mIoU	69.5	70.0	70.0	70.3	70.2	67.7

Table 10: Different strategies of time schedule.

Time Schedule	linear	cosine	sigmoid
mIoU	69.8	70.2	70.3

Table 12: Results on SYN. \rightarrow CS built with extended versions.

Method	base	B	M
DAFormer [38]	60.9	63.1	62.6
HRDA [39]	65.8	68.0	67.7
MIC [40]	67.3	68.7	68.2

G Influence of Time Schedule

We study different choices of time schedules for β_t , namely, linear [37], cosine [65], and sigmoid [44], with the same setting as Sec. F. The results are summarized in Tab. 10. Although selecting the appropriate schedule is significant for generating high-quality images in the diffusion model, it is robust in DiDA, and we can achieve consistently good performance among these strategies.

H Degradation-Based Domain Bridging

To further investigate the feasibility of our proposed motivation and provide deeper insight into the domain bridging mechanism, we conduct a quantitative analysis of the distribution discrepancy between domains. Specifically, we train models independently within different distribution spaces and evaluate their performance in terms of mIoU under both fully supervised and UDA settings, as shown in Fig. 7(a).

To better assess the degree of domain adaptation, we further report the relative performance in Fig. 7(b), defined as the ratio of UDA mIoU to the fully supervised counterpart at each degradation level. As the level of image degradation increases, we observe a gradual improvement in the relative performance, suggesting that the adaptation capability is enhanced. This indicates that domain-shared information is better preserved in the intermediate domains constructed via degradation.

However, image degradation inevitably destroys fine-grained visual details, which may include essential semantic cues. As a result, the semantic shift problem arises, where the corrupted features impair the discriminative power of the model and hinder further performance gains in UDA.

Our proposed DiDA framework addresses this issue by explicitly disentangling and compensating for the semantic shift through a diffusion-based encoder and reconstruction loss. This design enables the network to retain domain-invariant representations while mitigating the adverse effects of degradation, thereby achieving consistently better adaptation performance.

I More Results with Extended Versions

We further conduct more experiments about **Blur (B)** and **Mask (M)** built with DAFormer [38] and HRDA [39] and evaluate the performance on two benchmarks as shown in Tab. 11 and Tab. 12. These extended versions show consistent gains beyond all baselines, which further demonstrates the generality and expansibility of our framework.

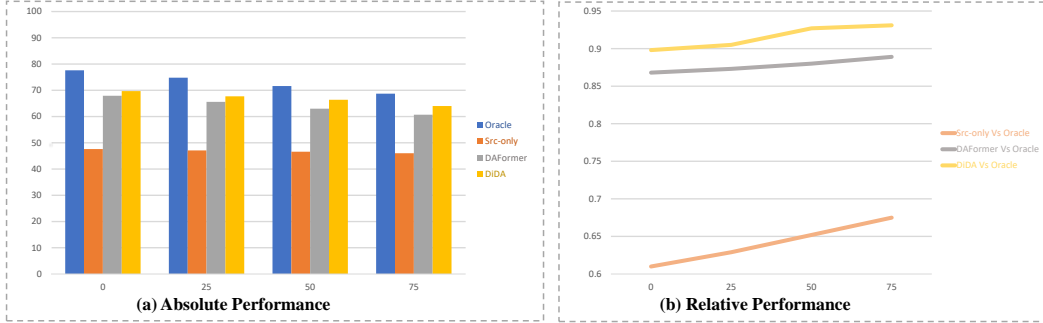


Figure 7: (a) The absolute performance of fully supervised learning and UDA settings (source-only, DAFormer [38] and DiDA) when the proportion of noise increases. Note that we train the models separately within different intermediate domains for the first three methods, while DiDA is trained only once and tested within different distributions. (b) Compared to oracle, the relative performance of UDA settings gradually improves, which means that the model’s adaptability is strengthened in these intermediate domains.

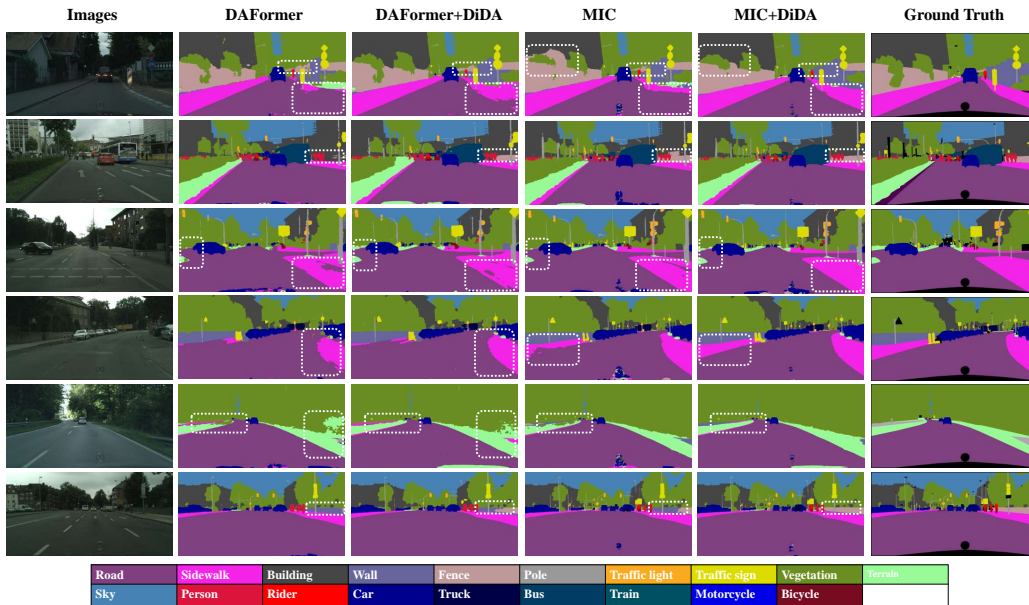


Figure 8: Qualitative comparison built with DAFormer and MIC. The dotted boxes mark regions improved by DiDA.

J Qualitative Results

In Fig. 8, we illustrate the qualitative comparisons of our DiDA against DAFormer and MIC. The previous methods fail to identify some classes on the target domain when their visual textures are significantly different from the source domain and confuse them with other visually similar classes (e.g., *sidewalk* and *road*, *fence* and *building*, *terrain* and *vegetation*). In this case, DiDA makes the model recognize semantic categories more dependent on context information, resulting in improved cross-domain performance.

K Visualization of Reconstruction Results

We visualize examples of reconstruction results in Fig. 9 with $t = 25, 50, 75$ in the time embedding module. The model can yield the best reconstruction results for degraded images with the corresponding t value. A fixed value of t leads to inadequate denoising for higher levels of degradation

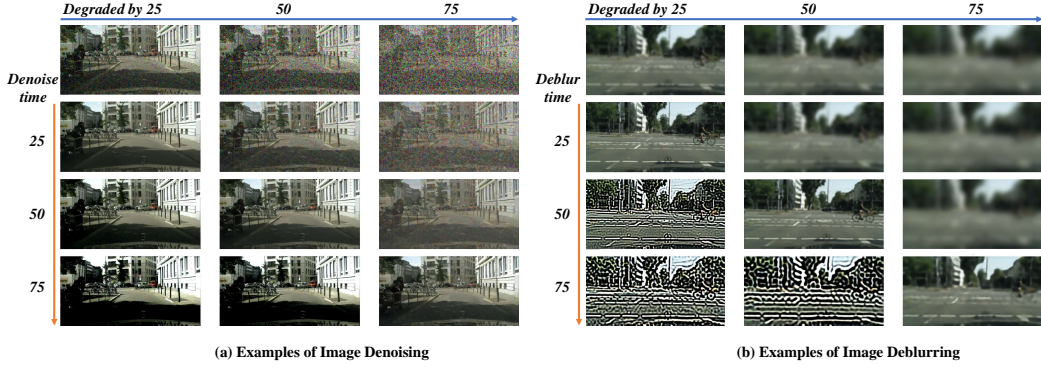


Figure 9: The examples of image reconstruction results with fixed diffusion time $t = 25, 50, 75$ as input in the time embedding module, where the image is degraded by 25, 50, and 75, respectively.

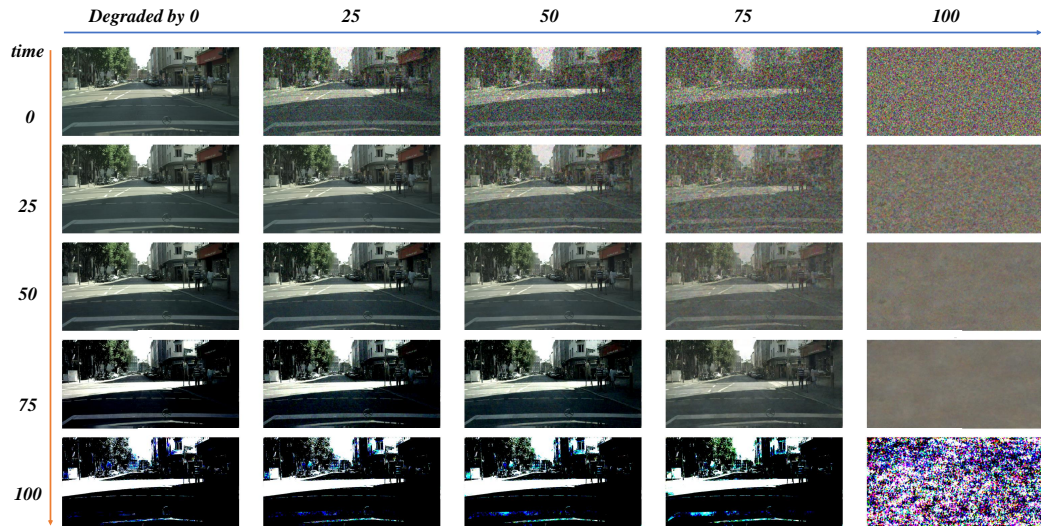


Figure 10: Examples of image denoising, horizontal coordinate represents the level of image degradation, and vertical coordinate indicates the t used in the inference.

and excessive denoising for lower levels of degradation, meaning that degradation information is accurately encoded in the time embedding. This further alleviates the semantic shift phenomenon and facilitates adaptive learning from the disturbed image.

L More Examples for Image Reconstruction

In this section, we give further details, analysis, and examples of image reconstruction. For different versions of the implementation of DiDA, we execute the inference with different diffusion times t on varying levels of image degradation for qualitative analysis.

Image Denoising This is the default setting of DiDA, the noise ϵ' is predicted by network \bar{f}_θ firstly and used to reconstruct the image as:

$$x_0^R = \frac{1}{\sqrt{\alpha_t}}(x_t - \sqrt{1 - \alpha_t}\epsilon'_i). \quad (14)$$

The examples are shown in Fig. 10. The noised images can be restored most perfectly when the diffusion time t matches the level of degradation. We can observe that the higher value of t has a more powerful anti-noise ability, which is consistent with our experimental results previously stated.

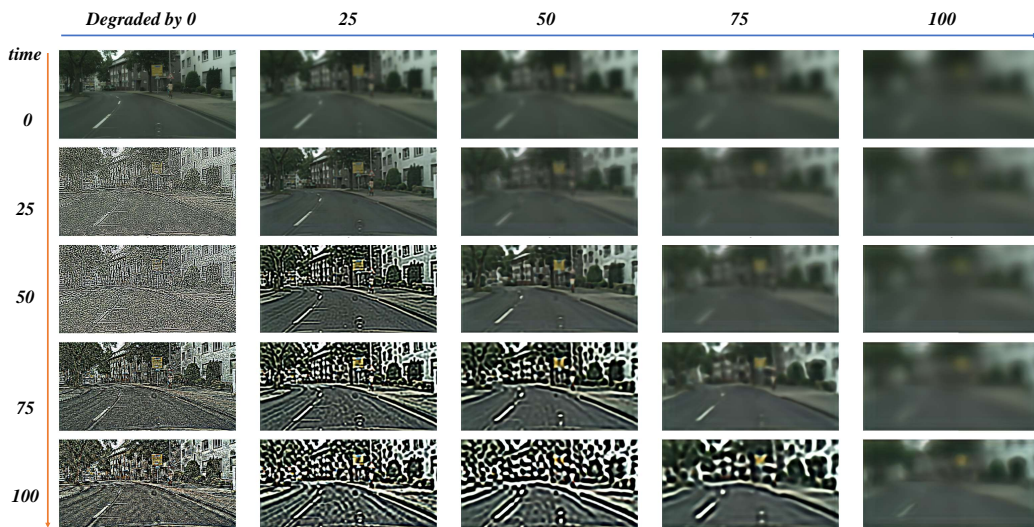


Figure 11: Examples of image deblurring, horizontal coordinate represents the level of image degradation, and vertical coordinate indicates the t used in the inference.

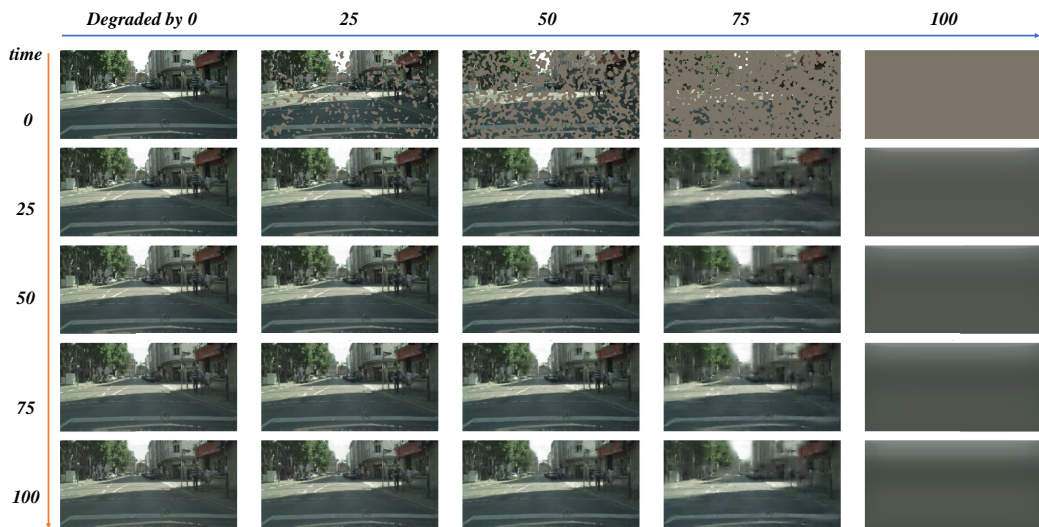


Figure 12: Examples of image inpainting, horizontal coordinate represents the level of image degradation, and vertical coordinate indicates the t used in the inference.

Image Deblurring. In the following two settings, the reconstructed image is directly predicted by \bar{f}_θ . Fig. 11 shows examples of image deblurring. We can draw a similar conclusion that the matched t achieves the best performance as above. The higher t results in excessive deblurring operation while the structure and edge information of the image are preserved, leading to more robust performance.

Image Inpainting. Fig. 12 shows examples of image inpainting. Unlike the former, when the variable t changes in the inference, the reconstruction quality for the masked image does not vary significantly. Since the mask operation is operated in a global view to control the ratio while the previous degrading operation is executed locally, it is difficult for the network to sense the level of degradation in this case. Therefore, DiDA achieves slighter performance gains with the implementation of mask operation.

M More Discussion with Domain Bridging

Directly transferring knowledge from the source domain to the target domain can be challenging due to significant discrepancies and pixel-wise gaps between the domains. To address this issue, some works propose gradually transferring knowledge by building a bridge between the source and target domains. This is achieved by constructing intermediate domains at the image level [64, 92, 94], feature level [22, 23, 58], or output level [41, 98]. One line of work utilizes style transfer techniques [16, 19, 30] to transfer the style of source data to target data, effectively creating intermediate domains. Another approach leverages data mix augmentation techniques [82, 102, 7], such as CutMix [96] and Mixup [97], to construct various intermediate domains. While these methods can effectively reduce the domain gap and facilitate the adapting ability of models, they have certain limitations. Style transfer-based methods are often dataset-specific and may generate unexpected artifacts, while data mix strategies can disrupt the contextual distribution of images and require intricate designs. Both approaches lack generalization ability and face the semantic shift problem, where the intermediate domains may not preserve the semantic information of the original domains. These limitations restrict their applicability in different scenarios. In contrast, our work aims to explore a universal and concise domain bridging strategy that can be easily integrated into existing UDA frameworks while explicitly compensating for the discriminative representations. By constructing intermediate domains through a diffusion forward process, we propose a dataset-agnostic approach that alleviates the semantic shift problem and enhances the generalization ability of the model.

N Limitation and Societal Impact

Our work presents a general and modular approach for domain adaptive semantic segmentation. While our method demonstrates consistent improvements across multiple UDA baselines and datasets, it still presents a few limitations. First, DiDA introduces moderate computational overhead during training due to additional modules such as the degradation encoder and reconstruction losses. Although we provide a memory-friendly variant, further optimization is needed for extremely resource-constrained environments. Second, the choice and combination of degradation operations are currently heuristic and manually designed; automating or learning this selection process could further enhance performance and generality.

This work focuses on domain adaptive semantic segmentation, a key area in computer vision with broad applicability in domains such as autonomous driving, medical imaging, and remote sensing. At present, we are not aware of any direct negative societal impacts associated with the proposed method.